Journal of Medicinal Chemistry

Article

pubs.acs.org/jmc

Structural Characteristics of Chloroquine-Bridged Ferrocenophane Analogues of Ferroquine May Obviate Malaria Drug-Resistance Mechanisms

Paloma F. Salas,[†] Christoph Herrmann,[†,‡] Jacqueline F. Cawthray,[†] Corinna Nimphius,[†] Alexander Kenkel,[†] Jessie Chen,[†] Carmen de Kock,[§] Peter J. Smith,[§,∥] Brian O. Patrick,[†] Michael J. Adam,[⊥] and Chris Orvig*[,†]

[†]Medicinal Inorganic Chemistry Group, Department of Chemistry, University of British Columbia, 2036 Main Mall, Vancouver, British Columbia V6T 1Z1, Canada

[‡]Advanced Applied Physics Solutions, 4004 Wesbrook Mall, Vancouver, British Columbia V6T 2A3, Canada

[§]Department of Medicine, University of Cape Town Medical School, Observatory 7925, South Africa

[∥]Department of Chemistry, University of Cape Town, Rondebosch 7701, South Africa

[⊥]TRIUMF, 4004 Wesbrook Mall, Vancouver, British Columbia V6T 2A3, Canada

Supporting Information

ABSTRACT: Five compounds displaying an unprecedented binding mode of chloroquine to ferrocene through the bridging of the cyclopentadienyl rings were studied alongside their monosubstituted ferrocene analogues and organic fragments. The antiplasmodial activity was evaluated against strains of the malaria parasite (*Plasmodium falciparum*). While the chloroquine-bridged ferrocenyl derivatives were less active than their five monosubstituted ferrocenyl analogues, they retained activity in the drug-resistant strains. The biological and physical properties were correlated to antiplasmodial activity. Intramolecular hydrogen bonding was associated with increased antiplasmodial action, but it is not the determining factor. Instead, balance between lipophilicity and hydrophilicity had a greater influence. It was found that calculated partition coefficient (log *P*) values of 4.5−5.0 and topological polar surfaces area (tPSA) values of ∼26.0 Å^2 give the best balance. The particular conformation, compact size, and lipophilicity/hydrophilicity balance observed in the bridged compounds provide them with the structural characteristics needed to escape the mechanisms responsible for resistance.

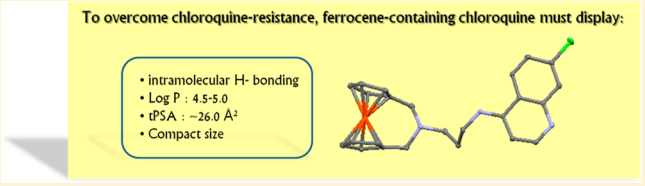

INTRODUCTION

Despite decades of research invested in its prevention and treatment, malaria remains one of the main causes of mortality and morbidity in the world. As reported by the World Health Organization (WHO), 3.3 billion people (almost half of the world population) were at risk of malaria in 2011.[1] A new study has revealed how the most recent peak of the disease was in 2004, taking the lives of 1 817 000 that year only.[2] With no vaccine available, malaria prophylaxis, diagnosis, and treatment are the only current approaches to the problem. The ability of the parasite (*Plasmodium falciparum*) to promptly develop resistance against antimalarial treatment has hindered the treatment of this disease. Malaria therapy has relied heavily on the use of artemisinins since early 2000. Unfortunately, reports of artemisinin resistance have surfaced since 2009,[3] perhaps foreshadowing the collapse of the current drug treatment.

Ferroquine (FQ, Chart 1) demonstrated an exceptional ability to overcome the resistance to the parent drug chloroquine.[4,5] Ferroquine is highly active against several strains of chloroquine sensitive and chloroquine resistant *Plasmodium* parasites in vitro and in vivo[4−8] and has recently completed phase IIb clinical trials.[9] Several ferrocenyl analogues of chloroquine, in an exploration of different connectivities between the ferrocene and the chloroquine moieties, have been synthesized and studied.[5−7,10−13] A representative group is included in Chart 1, and a complete set of FQ analogues have been reviewed elsewhere.[14−16]

The mechanism of action of ferroquine has been studied.[17,18] Although it is only partially understood, it is estimated to resemble to some extent that of the parent drug chloroquine. Like chloroquine, ferroquine is thought to interrupt the formation of hemozoin, the detoxification product of the free heme that results from the degradation of human hemoglobin during the intraerythrocyte stage of the disease. The buildup of large concentrations of heme perturbs the barrier properties of cellular membranes, causing electronic and membrane stress, disturbing ion homeostasis, and eventually causing the destruction of membranes and parasite death.[19] The increased therapeutic effectiveness of ferroquine has been attributed to its

Received: September 29, 2012

   dx.doi.org/10.1021/jm301422h | J. Med. Chem. XXXX, XXX, XXX−XXX

Chart 1. Ferroquine (FQ) and a Selection of Known Structural Analogues

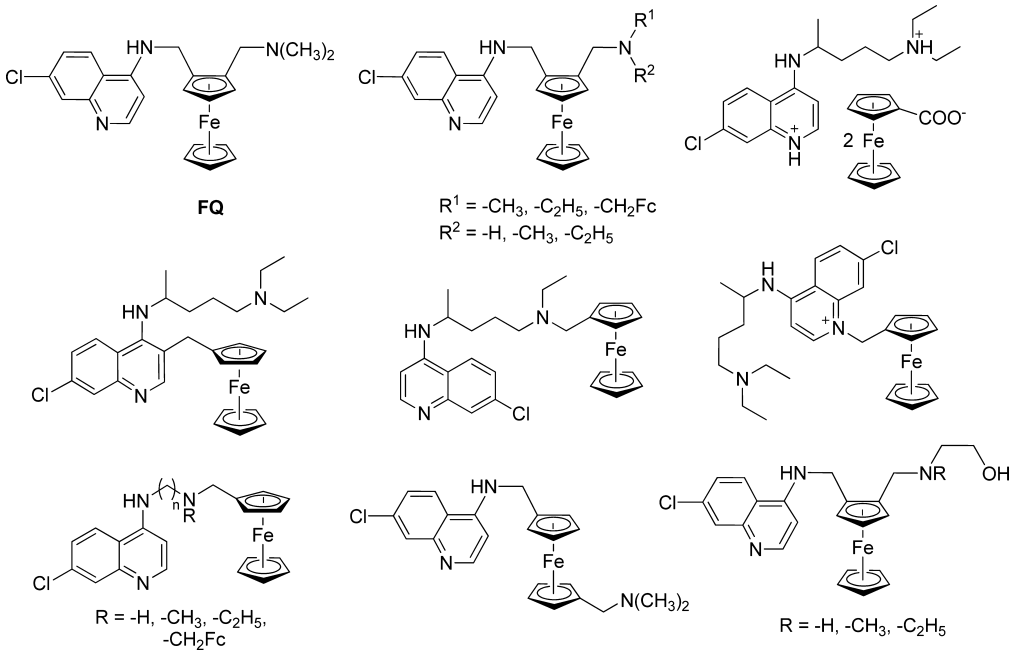

Chart 2. Chloroquine Derivatives (Series 3), Monosubstituted Chloroquine Ferrocenyl Compounds (Series 4), and 1,1′-Disubstituted Bridged Chloroquine Ferrocenyl Conjugates (Series 5)

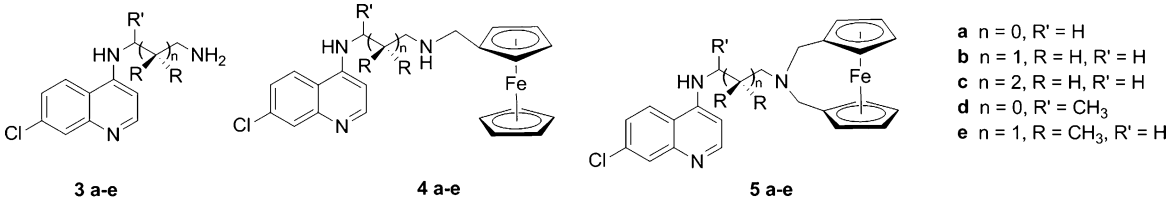

greater accumulation in the parasite food vacuole compared to that of the parent drug CQ.[20] In addition to thwarting the formation of hemozoin, ferroquine creates oxidative stress due to the redox activity of the ferrocene/ferrocenium pair.[20−22] After reaching its site of action, FQ acts first as a strong inhibitor of β-hematin formation (even more potent than CQ) and second as redox activator generating reactive oxygen species (ROS) via a Fenton-like reaction, irreversibly damaging the parasite.[20−22]

Ferroquine's weaker basic properties, higher lipophilicity, and conformation, influenced by the presence of an intramolecular hydrogen bond, allow this compound better permeation through membranes and therefore a higher accumulation at the site of action inside the parasite while targeting the lipophilic site of hemozoin formation more efficiently.[17,18,21,23] Despite structural similarities to chloroquine and ferroquine, none of the ferroquine analogues were able to outdo FQ in performance and, possibly more importantly, studies have not been able to explain unequivocally the role of the iron and how it contributes to the overcoming of resistance when ferrocene is bound to chloroquine. This has made apparent that a very structurally specific set of characteristics in ferroquine gives this compound the specificity necessary to escape the mechanisms that encompass chloroquine resistance. The exploration of the structural features that make ferroquine escape the resistance mechanisms remains incomplete and is of utmost importance, since more rational drug designs will be needed urgently if resistance to current antimalarials continues to grow worldwide.

In this study, two sets of ferrocenyl chloroquine conjugates with two distinct substitution patterns (series **4** and **5**) were synthesized using 4-aminoquinolines (series **3**) (Chart 2). Both series of ferrocenyl compounds (**4** and **5**) are structural analogues of ferroquine; the monosubstituted ferrocenyl 4-aminoquinoline derivatives (**4a−e**) present a ferrocene moiety covalently attached at the end of the *N*-alkylamino side chain of the 4-aminoquinoline, while compounds **5a−e** incorporate the same elements of series **4** in a more closed conformation, showcasing a previously unexplored mode of substitution, with the chloroquine derivative bridging together both cyclopentadienyl rings of the ferrocene (Chart 2), forming a ferrocenophane. The difference in conformation, flexibility, lipophilicity, and hydrophilicity of these compounds will illustrate the impact of these characteristics on the potency and ability of these ferroquine analogues to overcome drug resistance.

The antiplasmodial activity of these compounds (series **4** and series **5**) was studied with those of the respective organic quinoline fragments (**3a−e**), 4-aminoquinolines with an alkyl side chain of four or less carbon atoms, both linear and branched. It has been observed that 4-aminoquinoline derivatives of chloroquine containing side alkyl chains of altered lengths can retain the antiplasmodial activity of the parent drug against certain chloroquine-resistant strains of *Plasmodium falciparum*.[24−26] The number of carbon atoms between the two nitrogens in the diaminealkane side chain is a major factor for activity against chloroquine-resistant parasite strains.[27,28] Compounds presenting a shorter rather than longer

dx.doi.org/10.1021/jm301422h | J. Med. Chem. XXXX, XXX, XXX−XXX

Scheme 1. General Route for the Synthesis of Bridged Ferrocenyl 4-Aminoquinoline Derivatives (5a−e)[a]

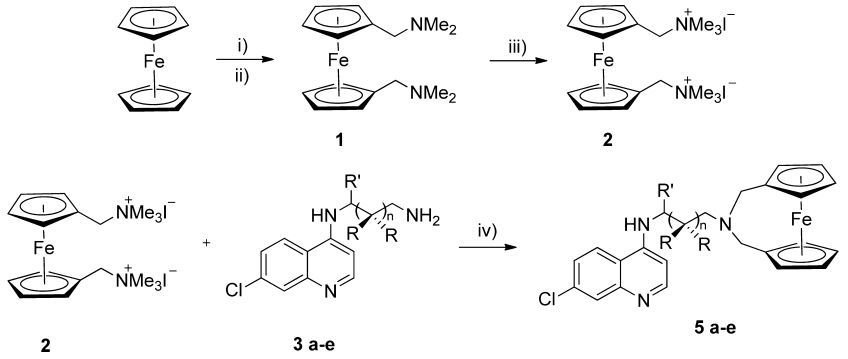

[a](i) *n*-BuLi, TMEDA, hexanes, 12 h, rt; (ii) $CH_2{=}N(CH_3)_2{}^+I^-$, THF, 10 min reflux, 24 h rt; (iii) MeI, MeOH, 10 min reflux; (iv) NaOH, CH_3CN, 6 h at 110 °C (in microwave reactor).

side chain tend to be more active, especially those with propyl[27,29] and butyl[30,31] alkyl chains. Several of the monosubstituted ferrocenyl 4-aminoquinoline derivatives (**4a−e**) have been studied in the past[7] and were taken here as a point of reference to develop a robust comparison with the bridged ferrocenyl 4-aminoquinoline derivatives (**5a−e**).

Structure−activity relationships were established by correlation of the antiplasmodial activity with other biological and physicochemical properties. These correlations were carried out in order to elucidate the structural factors that determine the antimalarial action of ferrocenyl chloroquine derivatives.

RESULTS AND DISCUSSION

Synthesis. The synthesis of each 4-aminoquinoline chloroquine derivative (**3a−e**) from the commercially available 4,7-dichloroquinoline and the corresponding alkyldiamine was as previously described[30,32] with slight modifications. These syntheses were carried out using a microwave reactor, reducing considerably the reaction time when compared to traditional methods. The monosubstituted ferrocenyl 4-aminoquinoline derivatives (**4a−e**) were prepared following methodology previously reported[7] with slight modifications. These compounds were formed via a reductive amination between commercially available ferrocenecarboxaldehyde and the corresponding 4-aminoquinoline derivatives **3a−e**.

The bridged ferrocenyl 4-aminoquinoline derivatives (**5a−e**) were formed by the condensation reaction of 1,1′-bis(*N*,*N*′-trimethylaminomethyl)ferrocene iodide (**2**) and the corresponding 4-aminoquinoline derivatives **3a−e** (Scheme 1). The nucleophilic displacement of the trimethylammonium group using the 4-aminoquinoline in the presence of a base is a known reaction for ferrocene substrates[33] with yields of up to 80% when employing conditions similar to those used here.[34,35] The trimethylammonium methylferrocene iodide is known to be an excellent electrophile due to the good leaving group property of the trimethylamine. Methodologies using conventional heat methods and a microwave reactor were used, with the latter method being advantageous because it reduces the reaction time by 8-fold. The average yield obtained was 20% (except for **5e**). The use of up to 10 equiv of softer bases such as pyridine and sodium carbonate yielded approximately half the amount of product. When a stronger base such as NaH was employed, no product was obtained. Instead, an unidentified ferrocenyl product (not containing the quinoline fragment) was observed on the column, possibly a product of decomposition during the reaction. The use of a protic solvent such as methanol resulted in no product as observed by LR-MS. Compound **5e** was obtained in a 3−5% yield. Unlike the other syntheses, the crude of **5e** contains more side products, thus the need for preparative TLC purification. We hypothesize that formation of **5** takes place by the stepwise attack of the primary terminal amine of the chloroquine derivative series **3** on the trimethylammonium groups of **2**. After the first attack of **3e** to **2**, a strong hydrogen bonding interaction turns the quinoline away from the other trimethylammonium group (as seen in the single crystal structure of the monosubstituted analogue **4e**[36]), hampering the second attack and displacement of the latter, resulting in lower yields for its formation. The synthesis of compound **5b** under a different methodology has been reported by others.[37] We offer here a simpler and more general methodology to produce these chloroquine ferrocenyl derivatives, as well as their full characterization and detailed study of physical and biological properties.

NMR Characterization. The influence of the two different bonding modes of chloroquine to the ferrocene moiety (in the compound series **4** and series **5**) was explored by ^1H and ^{13}C NMR spectroscopy. The ^1H NMR chemical shifts suffered by the 4-aminoquinoline hydrogens upon derivatization with ferrocene are interpreted as an alteration of the structural environment of the chloroquine-like molecule and thus as a potential alteration in the interaction (i.e., binding affinity) between the compound and the drug target hematin. The biggest deviation in NMR is observed for the secondary amine hydrogen at the aromatic heterocycle ($^1H{-}N_{Ar}$). This could potentially be related to the formation or removal of intramolecular hydrogen bonds between the NH proton in the 4-position of the quinoline ring and the N atom in the *β*-position to the cyclopentadienyl ring. Table 1 shows the ^1H NMR chemical shifts of the NH protons ($^1H{-}N_{Ar}$) expressed as $\Delta\delta$ (ppm) for the monosubstituted (**4a−e**) and the disubstituted (**5a−e**) compounds from the respective quinoline

Table 1. Comparison of the ^1H NMR Chemical Shifts of the $^1H{-}N_{Ar}$ Signals in the Quinolines 3a−e vs the Ferrocenes 4a−e and 5a−e[a]

	3a	3b	3c	3d	3e
$\Delta\delta$ (**4**), ppm	0.09	0.52	0.07	0.09	0.08
$\Delta\delta$ (**5**), ppm	0.38	−1.68	−0.78	0.53	−3.35

[a]$\Delta\delta$ is given in ppm, measured in $CDCl_3$, 400 MHz.

dx.doi.org/10.1021/jm301422h | J. Med. Chem. XXXX, XXX, XXX−XXX

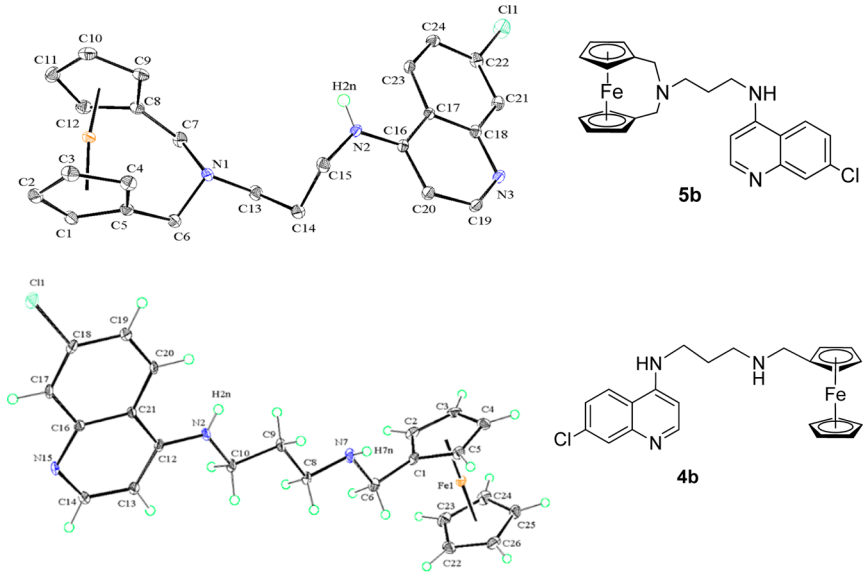

Figure 1. ORTEP diagrams for **5b** (top) and **4b** (bottom)[36] with 50% thermal ellipsoid level.

derivative **3**. A positive $\Delta\delta$ indicates the shifting of the $^1H-N_{Ar}$ to higher frequencies (lower field) upon coupling to ferrocene, and a negative $\Delta\delta$ indicates the shifting of the $^1H-N_{Ar}$ to lower frequencies (higher field).

The ^1H NMR signals of the $^1H-N_{Ar}$ proton are slightly shifted to higher frequencies in the respective monosubstituted ferrocene compounds with the C_2 side chain (**4a** and **4d**); however, upon formation of the bridging unit in **5a** and **5d**, the shift to higher frequencies is even more pronounced as shown in Table 1. This shift can be attributed to the deshielding effect of the formation of an intramolecular hydrogen bond between the aromatic NH and the alkyl N. The difference in the intensity can be explained as a consequence of the alkyl nitrogen being a secondary amine (in series **4**) and a tertiary amine (in series **5**). Compounds with a propyl or butyl chain (**b**, **c**, and **e**) present shifting to higher frequency upon single attachment of the quinoline derivative to ferrocene (series **4**), again indicating the formation of a hydrogen bond. However, when connected in the bridging fashion to ferrocene (series **5**), a very pronounced shifting to lower frequencies is observed. This could indicate that the hydrogen bonding is lost, possibly because of conformational restrictions in the geometry of **5b**, **5c**, and **5e**. The fact that the H-bonding in series **5** is maintained and even intensified when the length of the alkyl chain is $n = 2$ (branched or unbranched **5a** and **5d**) but is lost when the length of the alkyl chain is $n = 3$ or higher (**5b**, **5c**, **5e**) has been attributed to the distance between the NH-aromatic and the alkyl N groups that in **5a** and **5d** can be brought to close proximity, whereas in the longer chain analogues, the distance that separates these two groups does not allow the H-bonding.

For the ferrocene signals, the typical displacements for both types of substituted ferrocene are observed. In monosubstituted products (**4a**–**e**) one singlet is observed for the unsubstituted Cp ring, normally at δ 4.14–4.18 (ppm) and an AA′BB′-type spectrum with two triplets is observed for the $H_{\alpha,\alpha}'$ and $H_{\beta,\beta}'$ hydrogens in the substituted Cp ring. The hydrogens of the singly substituted cyclopentadienyl are located at lower field (compared to the Cp singlet) because of the electron withdrawing effect of the chloroquine derivative. As is expected for the disubstituted products (**5a**–**e**), two sets of triplets/multiplets are observed for the $H_{\alpha,\alpha}'$ and $H_{\beta,\beta}'$ hydrogens and the Cp singlet is absent. The only exception in the group is compound **5d**, whose nonsymmetric branched alkyl chain gives four different triplets for the substituted Cp rings. These peaks appear at higher field (4.02–4.20 ppm) in an effect opposite to that observed for the previous series **4**. This might be related to an electron donating effect of the nitrogen bridging both Cp rings. Spectroscopic characterization results with ^{13}C NMR spectroscopy is consistent with that from ^1H NMR.

X-ray Single Crystal Structure Characterization. The X-ray crystal structures and characteristic bond lengths and angles for the monosubstituted ferrocenyl compounds **4b** and **4e** were previously reported by our group.[36] In their solid state, the side chain orientation in **4e** brings the NH proton in the 4-position of the quinoline ring and the N atom in the β-position to the cyclopentadienyl ring to a close proximity so that intramolecular hydrogen bonding occurs at a distance of 2.11(2) Å, consistent with a hydrogen bonding interaction.[38] To allow a comparison of the solid state of the two types of ferrocene compound structures, the single crystal structures of compounds **4b** and **5b** are shown in Figure 1. The characteristic bond lengths and angles in **5b** are summarized in Table 2. Relevant bond lengths and angles in **4b** were previously reported by our group[36] and can be found in the Supporting Information. In **4b**, the distance between the corresponding N and H is 4.86 Å, ruling out the presence of an intramolecular hydrogen bond in the solid state. When compared to **4b**, **5b** presents significant differences in conformation. The quinoline ring and the ferrocene skeleton are parallel to each other but contained in two distinct planes, connected by a propyl chain that displays a nonstaggered arrangement with the quinoline ring almost perpendicular to the propyl chain. The quinoline ring is perpendicularly oriented to the plane that contains the cyclopentadienyl rings of the ferrocene, and no intramolecular hydrogen bonding can be observed in **5b**.

Another interesting characteristic of **5b** is that it is a strained ferrocenophane, specifically an aza[3]ferrocenophane. As expected for a ferrocene with an ansa [3] bridge, the normal geometry of ferrocene has been affected. The parameters used to describe this type of structure are listed in Table 3. The degree of ring tilt is expressed as the tilt angle (α), or the

dx.doi.org/10.1021/jm301422h | J. Med. Chem. XXXX, XXX, XXX–XXX

Table 2. Selected Bond Distances (Å) and Angles (deg) in 5b

	bond distance (Å)
C7−N1	1.4808(16)
C6−N1	1.4757(16)
N1−C13	1.4764(14)
C16−N2	1.3514(14)
N2−C15	1.4580(15)
$N2-H2_N$	0.8800
	angle (deg)
$H2_N-N2-C16$	118.6
C15−N2−C16	122.77(10)
C7−N1−C13	109.70(10)
C13−N1−C6	109.03(9)
C6−N1−C7	111.12(10)
C8−C7−N1	113.01(10)
C5−C6−N1	114.36(10)
C13−C14−C15	112.14(10)
N1−C13−C14	112.29(10)
N2−C15−C14	113.98(10)
N1−C7−C8−C9	51.15(17)
C14−C15−N2−C16	−72.96(14)
N1−C13−C14−C15	−69.95(13)

Table 3. Structural Parameters of Strained Ferrocenophane Compound 5b

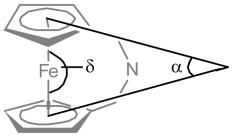

parameter	
α (deg)	12.12
δ (deg)	171.3(4)
$Cp_{centroid}-Cp_{centroid}$ (Å)	3.2517(2)
N deviation from C5−C6−C7−C8 (Å)	0.745
C6 deviation from Cp plane (Å)	0.138(2)
C7 deviation from Cp′ plane (Å)	0.120(2)

dihedral angle between the two planes that contain each of the Cp rings. The tilt angle (α) of 12.12° is not considered to induce high strain (tilt angles of up to 32° are considered to induce significant of strain).[39] This aza[3]ferrocenophane is structurally similar to a [3]ferrocenophane (a propane chain bridging the two cyclopentadienyl rings), since the latter has tilt angles up to 12.6°.[39] Ferrocenophanes in general are expected to show unique chemical properties due to the functionality in the side arm. Strain energy can be imbedded in this type of compound (**5a−e**) and that might be a focus of research, since this energy and the effects on its conformation could possibly influence antiplasmodial activity. Alternatively, the introduction of conjugated groups could tune the electronic character of the system. Aza[*n*]ferrocenophanes are known to undergo reversible electron transfer between the Fe and N atoms in the oxidized state.[40]

In Vitro Antiplasmodial Activity Studies. The antiplasmodial activities of the compounds **3a−e**, **4a−e**, and **5a−e** were evaluated in vitro against the chloroquine-sensitive (CQS) D10 and the chloroquine-resistant (CQR) Dd2 and K1 strains of *P. falciparum*. The activities of these compounds were compared to the reference drug chloroquine (CQ). A full dose−response was performed for all compounds to determine the concentration inhibiting 50% of parasite growth (IC_{50}). The results are presented in Table 4. The activities of certain compounds in the second chloroquine-resistant strain (K1) could not be measured because of insufficient sample to carry the testing of all compounds in parallel.

All disubstituted bridged ferrocenyl compounds **5a−e** demonstrated activity against all the tested parasite strains. The most active compound of this group is **5c** with IC_{50} values of 91.3 and 152.2 nM in the parasite strains D10 and Dd2, respectively. On average, compounds **5a−e** are more active in the Dd2 (CQR) strain. When compared against the control, **5a−e** are less active than chloroquine against D10 (CQS), as expected. However, **5a**, **5b**, and **5c** demonstrate more activity than chloroquine against Dd2 (CQR), as did **5b** and **5d** against K1 (CQR), overcoming the parasitic resistance associated with

Table 4. In Vitro Antiplasmodial Activity and Resistance Indices against *P. falciparum* CQS D10, CQR Dd2, and CQR K1 Strains[a]

compd	IC_{50}, CQS D10 (nM)	IC_{50}, CQR Dd2 (nM)	RI [b]	IC_{50}, CQR K1 (nM)	RI [c]
3a	36.1 ± 13.5 (*n* = 2)	261.6 ± 18.0 (*n* = 2)	7.3	ND	
3b	50.9 ± 29.7 (*n* = 2)	398.8 ± 42.4 (*n* = 2)	7.8	ND	
3c	76.1	1697.8 ± 20.0 (*n* = 2)	22.3	ND	
3d	29.7 ± 17.0 (*n* = 2)	80.6 ± 42.4 (*n* = 2)	2.7	160.1 ± 59.4 (*n* = 3)	5.3
3e	15.2 ± 7.6 (*n* = 2)	30.3 ± 15.2 (*n* = 2)	2.0	72.0 ± 0.76 (*n* = 3)	4.8
4a	60.8	35.7 ± 4.76 (*n* = 2)	0.6	1467.6	24.1
4b	138.3	297.4 ± 69.2 (*n* = 2)	2.2	16.1	0.1
4c	40.2	100.5 ± 22.3 (*n* = 2)	2.5	114.1 ± 35.7 (*n* = 3)	2.8
4d	43.8 ± 20.7 (*n* = 2)	23.1 ± 4.6 (*n* = 2)	0.5	260.5 ± 87.6 (*n* = 3)	5.9
4e	368.1	1136.8 ± 21.6 (*n* = 2)	3.0	90.9	0.3
5a	176.0	129.7 ± 23.2 (*n* = 2)	0.7	ND	
5b	323.0	224.3 ± 6.73 (*n* = 2)	0.7	307.3 ± 170.5 (*n* = 3)	0.9
5c	91.3	152.2 ± 6.52 (*n* = 2)	1.6	ND	
5d	444.2	269.2 ± 4.48 (*n* = 2)	0.6	291.6 ± 2.24 (*n* = 3)	0.7
5e	669.0	506.5 ± 21.1 (*n* = 2)	0.7	ND	
FQ	18.0[14]	19.0[14]	1.06	14.0[14]	0.8
CQ	29.1 ± 7.75 (*n* = 19)	180.3 ± 77.4 (*n* = 15)	6.2	758.0	26.0

[a] *n* = number of data sets averaged. ND = not determined. [b] Resistance index (RI) = IC_{50}(Dd2)/IC_{50}(D10). [c] Resistance index (RI) = IC_{50}(K1)/IC_{50}(D10).

dx.doi.org/10.1021/jm301422h | J. Med. Chem. XXXX, XXX, XXX−XXX

the quinoline fragment. The monosubstituted ferrocenyl compounds **4a−e** also demonstrate activity in both CQS and CQR strains of *P. falciparum*. The most active compounds against Dd2 are **4a** and **4d**, while the most active compounds against the K1 strain are **4b** and **4e**. Unlike series **5**, these compounds are generally more active in the CQS D10 strain than in the CQR Dd2 and K1. The organic components, the chloroquine derivatives **3a−e**, demonstrate a profile similar to that of chloroquine; they are active against D10 but lose activity against Dd2 and K1. The exceptions are the most active compounds **3d** and **3e**.

The activities of compounds in the series **4** and **5** are sensitive to the level of drug resistance of the parasite strains. The different responses observed against Dd2 and K1 may suggest some level of strain specificity on the activity of these compounds. Nevertheless, on average (excluding certain exceptions), activities of **5a−e** were superior in the resistant strains vs the sensitive strain while the opposite was observed for **4a−e** and **3a−e**.

The effects of the substitution on the chloroquine derivatives will be discussed in terms of each set of specific length of the methylene spacer. For the ethyl chain quinoline (**a**), while the ferrocenyl derivatives are less effective than the organic fraction **3a** in the CQS D10 strain, an improvement of 7-fold and 2-fold in the CQR Dd2 strain is observed for the monosubstituted ferrocenyl **4a** and for the bridged ferrocenyl **5a**, respectively. However, against the CQR K1 strain, **4a** loses all activity, becoming almost 2-fold less active than chloroquine itself. A similar situation is observed for the propyl (**b**) and butyl (**c**) chain derivatives. The ferrocenyl derivatives **4b** and **5b** are 1.3- and 2-fold more active than the organic component **3b** in the chloroquine-resistant Dd2 strain, respectively. Even more dramatically, **4c** and **5c** are 17 and 11 times more active than **3c** in the CQR Dd2 strain, respectively. A different trend is observed for the branched methylene spacer derivatives **d** and **e**. In the case of the isopropyl derivatives (**d**), the activity of the organic component **3d** is superior to that of the ferrocenyl derivatives against all strains except for **4d**. In the case of the 2,2′-dimethylpropyl derivatives (**e**), the activity of **3e** is far superior to that of the ferrocenyl derivatives in both D10 and Dd2 strains but almost equal against K1. **3e** is up to 44 times more active than **5e** in D10 and 38 times more active than **4e** in Dd2. It was found then that the length of the methylene spacer was not as strong an influence in the activity as is the degree of branching. These results illustrate a different activity trend for the linear and the branched quinoline derivatives: linear derivatives can overcome chloroquine resistance by derivatization with ferrocene; however, the bulkier branched derivatives lose all activity when derivatized with ferrocene. Even though ferroquine (FQ) was not used as control during this experiment, IC_{50} values in these parasite strains have been reported in literature.[14] Ferroquine has IC_{50} values of 18, 19, and 14 nM in the chloroquine sensitive strain D10 and the chloroquine resistant strains Dd2 and K1, respectively.[14] A number of the averaged values of the antiplasmodial activity were obtained with uncertainty reflected in the discrepancy between independent screenings of the compounds. Diverse factors beyond our control contribute to this inconsistency. These include the use of human blood for parasite culture, where the age and source vary in almost every assay performed, the use of synchronized or nonsynchronized cultures, the parasitemia and hematocrit levels that can give rise to a greater or lesser innoculum effect, and the fact that some compounds were tested as suspensions.

The resistance index (RI) provides a valuable tool for analysis of drug candidates. Small RI values indicate activity regardless of the susceptibility of the parasite strain. On the contrary, large values indicate loss of activity due to resistance development or likelihood of resistance development. A promising drug lead will necessarily have a small resistance index as a sign of not being detected by whatever resistance mechanism is operating. RI values for each compound ranged from 0.5 to 24.7 (Table 4). As expected, the quinoline derivatives **3a−e** showed the largest tendency to develop resistance due to their structural similarity to chloroquine. The lowest values of RI were found for the disubstituted bridged ferrocenyl compounds **5a−e** (Table 4). Figure 2 illustrates the resistance index calculated for these compounds for the parasite strains CQS D10 and CQR Dd2. The diagonal line represents an equal antiplasmodial potency regardless of the chloroquine susceptibility of the strain (RI = 1). Ferroquine (FQ), for example, not only displays low IC_{50} values for both parasite strains but also has an RI value close to 1,[14] which makes this compound very attractive as an antiplasmodial drug lead. Compounds **5a−e** are not as potent as FQ but remain close to the ideal line, unlike compound series **3** and **4** that are more potent but develop resistance later. The fact that some of these compounds are equally or more potent in drug-resistant parasite strains than in drug-sensitive strains suggests that, rather than following the mechanism of accumulation of chloroquine, these are following a different mechanism allowing them not to be detected by the transmembrane proteins responsible for lower accumulation of the drug (origin of resistance). Ferroquine indiscriminative action in parasite strains has been explained in a similar fashion.[18,41]

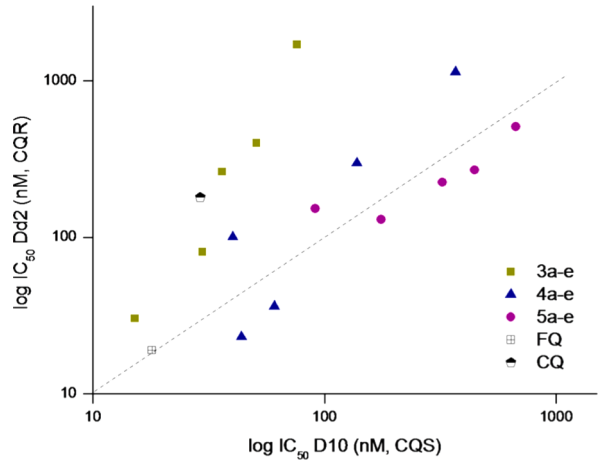

Figure 2. Resistance index (RI) expressed as the correlation of the in vitro antiplasmodial activity against *P. falciparum* CQS D10 and CQR Dd2 parasite strains.

In Vitro Antitumor Activity and Cytotoxicity Assay. The toxicity of the compounds was assessed in vitro. Two human cell lines originally from human breast tissue were employed. The normal breast epithelial cells MCF-10A (CRL-10317) and the breast cancer cells MDA-MB-435S (HTB-129) were used as references for a healthy and cancerous cell line, respectively. Chloroquine and other quinoline-containing drugs traditionally used as antimalarials have also been studied as anticancer agents in human breast tissue.[42] Antitumor activity

dx.doi.org/10.1021/jm301422h | J. Med. Chem. XXXX, XXX, XXX−XXX

and cytotoxicity were assayed using the MTT methodology.[43] Cisplatin (cis-diamminedichloroplatinum(II)) was used as a positive control for cell death. Chloroquine and ferroquine were also used as control. All tested compounds were found to lower the viability of the tested cell cultures, with increasing detrimental effect with increasing compound concentration. IC_{50} values calculated for all tested compounds are shown in Table 5.

Table 5. Toxicity of the Compounds (Expressed as IC_{50}) against the Human Normal Breast Epithelial Cell Line MCF-10A and the Human Breast Cancer Cell Line MDA-MB-435S

	IC_{50} (μM)	
compd	MCF-10A	MDA-MB-435
3a	74.7 ± 3.7	17.5 ± 1.4
3b	103.0 ± 6.0	21.90 ± 1.3
3c	47.9 ± 1.4	13.56 ± 2.4
3d	107.0 ± 2.1	25.67 ± 0.7
3e	105.3 ± 3.1	22.71 ± 1.2
4a	4.1 ± 0.5	3.1 ± 0.2
4b	2.8 ± 0.3	3.1 ± 0.1
4c	3.8 ± 0.6	3.0 ± 0.2
4d	5.5 ± 0.1	3.2 ± 0.1
4e	5.4 ± 0.1	2.6 ± 0.1
5a	2.4 ± 0.2	1.7 ± 0.1
5b	4.0 ± 1.0	3.1 ± 0.3
5c	4.2 ± 0.9	2.8 ± 0.2
5d	1.4 ± 0.1	1.4 ± 0.1
5e	0.3 ± 0.1	0.6 ± 0.1
cisplatin	11.1 ± 1.5	92.3 ± 19.8
FQ	26.5 ± 2.0	12.3 ± 0.8
CQ	69.7 ± 4.8	20.2 ± 1.2

In the normal breast epithelial cell line MCF-10A, the chloroquine derivatives **3a–e** are mild to nontoxic. Once derivatized with ferrocene, the series of compounds **4a–e** and **5a–e** show a noticeable increase in toxicity. Against the breast cancer cell line MDA-MB-435S, **3a–e** are more active, with IC_{50} values that are roughly a fifth of the values displayed in the normal MCF-10A cell line. The IC_{50} values obtained for the series of compounds **4a–e** and **5a–e** against the MDA-MB-435S cell line are similar to those obtained for the normal MCF-10A cell line, indicating that any effect is mainly driven by the toxicity associated with the compounds.

In general, the addition of the metallocene fragment increases greatly the toxicity of the compounds, and this is comparable to what has been observed for other ferrocene chloroquine compounds.[36,44,45] However, FQ seems to be somewhat less toxic than the compounds on series **4** and **5**. The mode of substitution, either monosubstituted in one ferrocene ring or in the bridged form, does not seem to have a direct influence on the overall activity of the compounds and neither does the length of the side chain or its degree of branching. Although the ferrocenyl compounds were more toxic than cisplatin and chloroquine, these data only show the in vitro response to two cell lines. More extensive studies will be required to determine the toxicity profile of these compounds and thus their real appeal as pharmacophores.

Hematin Association Assay. Extensive evidence supports Fe(III)PPIX (hematin) as the molecular drug target of quinoline antimalarial drugs.[46] Most 4-aminoquinolines are thought to act by complexing Fe(III)PPIX, thus reducing its availability and incorporation into hemozoin and hence halting the detoxification process of the parasite.[28,46] For instance, monomeric Fe(III)PPIX and chloroquine form a $\pi-\pi$ complex[47,48] in neutral or weakly acidic media.[49] Thus, the antiplasmodial activity of 4-aminoquinoline compounds can be correlated to their ability to coordinate hematin, and this can be monitored through UV–vis methods. The $\pi \rightarrow \pi^*$ electronic transitions in the porphyrin ring give rise to a Soret band at 402 nm.[46] A strong hypochromism is then observed upon complex formation between the Fe(III)PPIX and the quinoline compound. This effect can be quantified and fitted to a model of association to determine the strength of complex formation.[46,50]

The formation of the complex between Fe(III)PPIX and the CQ derivative was monitored as a function of the change in absorbance of the Soret band of hematin at 402 nm upon coordination to the quinoline moiety. Figure 3 shows a set of

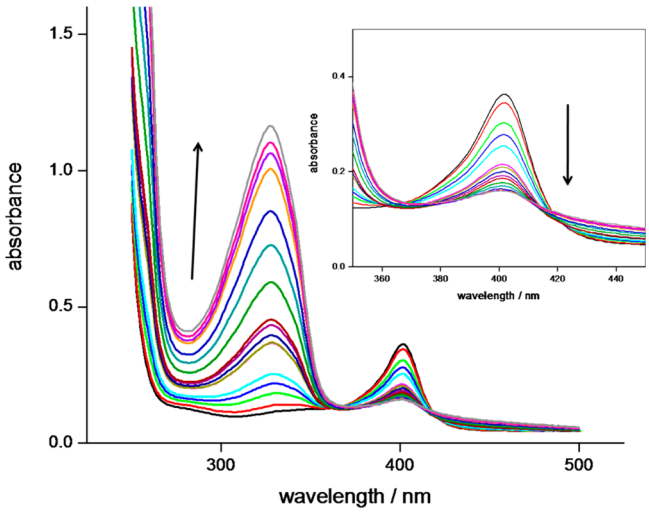

Figure 3. Spectroscopic changes observed when Fe(III)PPIX is titrated with compound **4a**.

spectra collected when the hematin solution was titrated with increasing concentrations of **4a**. The spectral changes observed show a decrease in the Soret band of Fe(III)PPIX at 402 nm and an increase in the quinoline band at around 338 nm that is explained by the increasing concentration of the quinoline derivative. The data obtained were fit to a 1:1 association model to calculate the association constant as log K. This 1:1 association model is the best fit model for the parent drug chloroquine under these conditions.[50] Titration data for a selection of compounds are shown in the Supporting Information. The association constants (as log K) calculated for the compounds are presented in Table 6.

All compounds interacted with Fe(III)PPIX. The association constants (log K) obtained for the quinoline fragments (**3a–e**) were, as expected, relatively high regardless of the length or branching of the side alkyl chain. These values are close to the value obtained for chloroquine that was used as a control in this study (log $K = 5.07 \pm 0.05$). The association constants for both **4a–e** and **5a–e** were on average lower than those observed for the organic fragments. Within the monosubstituted ferrocenyl compounds, **4a**, with an unbranched ethyl side alkyl chain, exhibits the highest value for this series (log $K = 4.71$). It was observed that a longer and more branched side alkyl chain

dx.doi.org/10.1021/jm301422h | J. Med. Chem. XXXX, XXX, XXX–XXX

Table 6. Association Constants (log *K*),[a] ClogP[b] and PSA[c] of 3a−e, 4a−e, and 5a−e in Their Neutral State

compd	log *K*	ClogP	PSA (Å^2)
3a	4.67 ± 0.05	1.27	51.4
3b	4.85 ± 0.02	1.38	51.0
3c	4.86 ± 0.04	1.83	51.0
3d	4.62 ± 0.05	1.59	51.0
3e	4.80 ± 0.03	2.49	47.5
4a	4.71 ± 0.03	4.48	38.7
4b	4.42 ± 0.10	4.84	39.0
4c	4.13 ± 0.05	4.83	38.9
4d	3.68 ± 0.04	4.79	36.0
4e		5.64	33.6
5a	4.18 ± 0.05	6.38	27.4
5b	4.23 ± 0.15	6.74	25.3
5c	4.76 ± 0.03	6.71	26.0
5d	4.47 ± 0.07	6.69	25.1
5e	4.41 ± 0.13	7.54	21.7
FQ	5.52 ± 0.03 [21]	5.1	26.2
CQ	5.07 ± 0.05	4.63	27.2

[a]Obtained from spectrophotometric titrations of Fe(III)PPIX with compounds **3a−e**, **4a−e**, and **5a−e** in 40% DMSO, apparent pH 7.5, 0.020 M HEPES buffer at 25 °C. [b]ClogP = calculated log *P*. [c]PSA = calculated polar surface area.

presented a lower value of log *K*. The association constant of compound **4e** could not be determined because of insolubility. Unlike compounds **4a−e**, the disubstituted bridged ferrocenyl compounds **5a−e** displayed log *K* values that increased with length and branching of the side alkyl chain. The highest association constant was obtained for compound **5c**, the unbranched butyl side chain (log *K* = 4.76). The different structural conformations for these two types of ferrocenyl substitution seem to alter significantly the association of the quinoline fragment with Fe(III)PPIX. In **5b**, the ferrocene fragment is twisted into close proximity to the quinoline fragment which could sterically hinder the $\pi-\pi$ association with Fe(III)PPIX, lowering the association constant. In **4b**, the ferrocene is directed further away from the quinoline fragment and hence does not disturb the quinoline fragment association with hematin, which is reflected in a higher value of log *K*. In turn, it is expected that the longer chain in the bridged derivative **5c** provides a less sterically hindered interaction which would explain the elevated log *K* value for **5c**. The association constant reported for ferroquine, log *K* = 5.52 ± 0.03,[21] and the value reported for CQ (log *K* = 5.52 ± 0.05)[28] and found in this study (log *K* = 5.07 ± 0.05) are still comparable to the values obtained for the association constants of both series of ferrocenyl derivatives.

***β*-Hematin Formation Inhibition Assay.** The antimalarial properties of these compounds were also explored as a function of their capacity to inhibit the formation of *β*-hematin (synthetic hemozoin). This was evaluated quantitatively using the pyridine hemochrome UV−vis assay.[51] In aqueous solutions of hematin, formation of the solid *β*-hematin is stimulated by addition of sodium acetate. The degree of inhibition of *β*-hematin formation achieved by the tested compound is measured by calculating the concentration of free hematin remaining at the end of the assay.[51,52] Hematin solution in 0.1 M NaOH was incubated in the presence of the studied compounds with increasing numbers of equivalents. *β*-Hematin formation was initiated by the addition of acetate solution to give a final concentration of 4.5 M and pH 4.5. After incubation at 60 °C for 1 h, the process was quenched by the addition of a 5% (v/v) pyridine solution and buffered at pH 7.5 to give the ideal conditions for the formation of a Fe(III)PPIX−pyridine complex with the hematin remaining in solution. The absorbance of the complex formed by Fe(III)PPIX and pyridine is measured at 405 nm. The relationship between absorbance and concentration is linear; higher concentrations of hematin in solution indicate the potent effect of the drug to divert the consumption of hematin from the formation of *β*-hematin.

A selection of collected spectra is shown in Figure 4. When no equivalents of the compounds are present, a small amount

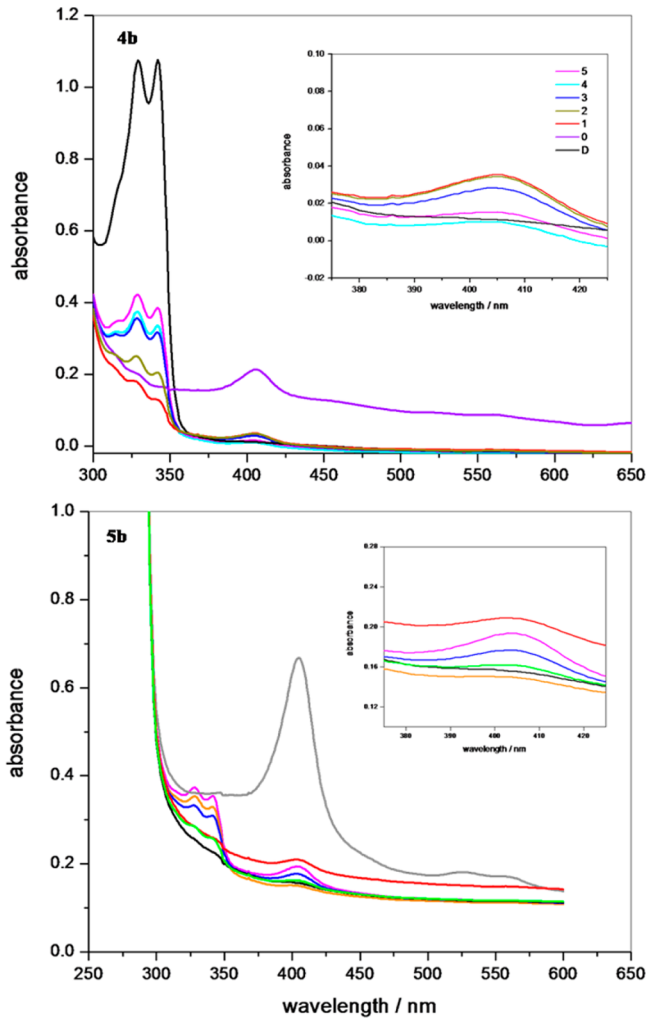

Figure 4. Interaction of pyridine and hematin present in solution after incubation for the formation of *β*-hematin. The sets of spectra correspond to increasing amounts of compounds **4b** and **5b**. The absorbance of the Soret band of the Fe(III)PPIX−pyridine complex occurs at 405 nm. The legend indicates the number of equivalents of test compound added in each experiment. D indicates drug only, a blank using the maximum concentration of drug in the 5% pyridine aqueous solution.

of hematin is observed; however, at any other number of equivalents, no absorbance is detected for this complex indicating that no free hematin is left in solution. The low absorbance of the Fe(III)PPIX−pyridine complex at 1 or 2

dx.doi.org/10.1021/jm301422h | J. Med. Chem. XXXX, XXX, XXX−XXX

equiv of the compound quickly decays after the number of equivalents increase. These could lead to false negative results. If these compounds do not inhibit formation of β-hematin, all spectra obtained would be expected to be identical to the spectra obtained at zero equiv of the compound. This phenomenon of quenching of the absorbance of the hematin that should remain in solution, even after a large portion of it has been used to form β-hematin, is explained by solubility restrictions. The weak inhibitory properties are related to the poor solubility of the compounds in aqueous media. The compounds in stock solutions, completely dissolved in DMSO, were added to the aqueous media where they could precipitate from large amounts of water. It has been noted that poorly water-soluble compounds trap unreacted hematin in the solid state.[51] This would explain the complete absence of the Fe(III)PPIX–pyridine complex absorbance peak. It is known that compounds with very low water solubility, such as the quinoline drug halofantrine, indeed inhibit β-hematin formation and appear to prevent solubilization of hematin in aqueous pyridine medium, giving false negative results.[51] Moreover, the cloudiness arising from partial precipitation of the compounds and/or from the transport of miniparticles of β-hematin can interfere with the measurement of absorbance. The use of other solvents to facilitate the dissolution of the studied products was not tested, since the solvent effect on this assay has not been explored and could considerably affect the interactions that cause the formation of β-hematin. The addition of other organic solvents could produce misleading results, since by analogy increasing the DMSO concentration in the association with hematin assay weakens the interaction of some aminoquinolines with Fe(III)PPIX.[53]

Partition Coefficient and Molecular Shape Analysis. Accumulation of chloroquine-based compounds in the parasite food vacuole lacks a special transport mechanism and is determined by physical characteristics that will allow the crossing of membranes and the retention upon protonation inside the vacuole.[49] Therefore, physical characteristics such as lipophilicity and hydrophilicity have been suggested to play a determining role in the accumulation of drugs inside the acidic food vacuole of the malaria parasite.[19,54,55] For ideal pharmacokinetic and pharmacodynamic properties in a drug, the ideal distribution coefficient is a moderate intermediate between hydrophilic and hydrophobic. The partition coefficient (log P) is used frequently to define the lipophilic character of a drug. Theoretically calculated values of log P (ClogP) are presented in Table 6, calculated using the commercially available ACDLABS 11.0 program.[56,57] In general these compounds are all lipophilic (log $P > 0$). Chloroquine derivatives **3a–e** experience, as expected, an increase in lipophilicity as the alkyl side chain increases in length and in branching. The calculated log P values show a considerably larger lipophilicity for compounds **4a–e** and **5a–e** compared to **3a–e**. The disubstituted bridged ferrocenyl compounds are 10^5-fold more lipophilic than the parent chloroquine fragment while the monosubstituted ferrocenyl compounds are 10^4 more lipophilic. This approximate 10-fold difference in lipophilicity between series **4a–e** and series **5a–e** arises exclusively from the difference in ferrocene substitution and structural orientation. The more closed conformation of the bridged compounds likely provides a more hydrophobic surface and therefore a higher value of log P. Within each of the ferrocenyl series, the lipophilicity of the first four members is relatively similar, but the 2,2′-dimethylpropyl side chain ferrocenyl derivative (**4e** and **5e**) is the most lipophilic of each group, as expected. These ClogP values are similar to those obtained for chloroquine (4.63) and for FQ (5.1).[17] The high lipophilicity of FQ has been postulated to be key in the good absorption and transport properties across cell membranes.[58]

Computational methods can be used to predict important pharmacophoric properties of drug candidates such as the ability of these compounds to permeate biological membranes[59] and have been used in the past to rationalize antimalarial activity.[17,21,60,61]

The molecular electrostatic potential (MEP) surface gives an indication of the charged surface area, its accessibility by polar solvents (giving also an idea of the hydrophilicity of the compounds), and an idea of the importance of the orientation of the molecule for the activity of the drug candidate. Therefore, MEP maps were generated to probe key structural features for the compounds such as steric, electrostatic interactions, hydrogen donor/acceptor properties, and lipophilicity. Figure 5 shows a comparison of the molecular electrostatic potential (MEP) surfaces generated for a selection of relevant studied compounds at the DFT-B3LYP level of theory for the neutral state.

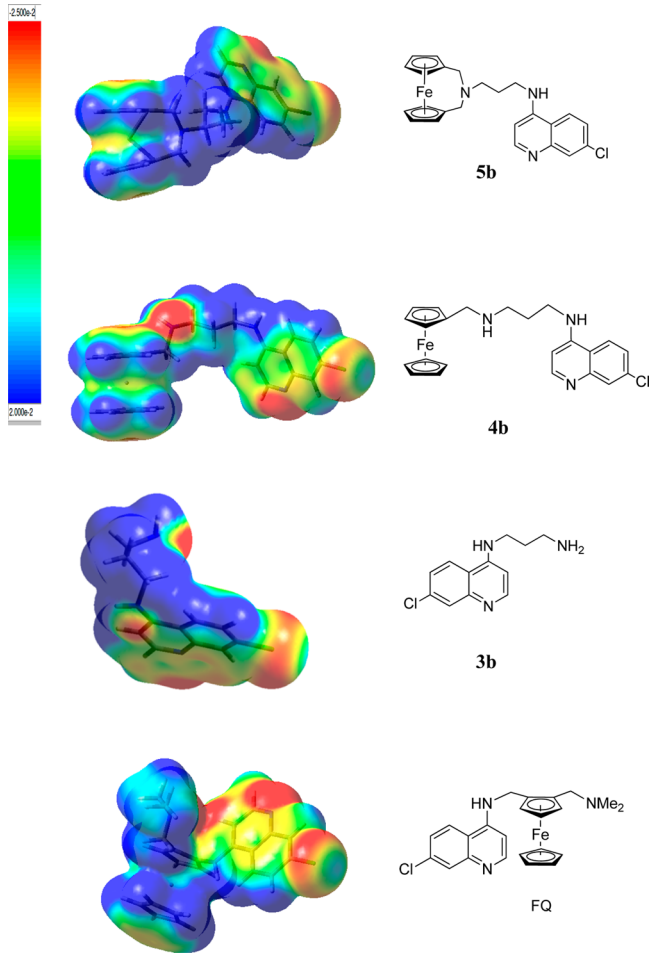

Figure 5. Comparison of the molecular electrostatic potential (MEP) surfaces of a selection of compounds from this study.

In a comparison of the MEP maps of the two modes of ferrocenyl substitution, exemplified by **5b** and **4b**, the most noticeable difference comes from the nitrogen that connects the alkyl chain and the ferrocene. In **4b**, this nitrogen is more electronically available with the lone pair probably oriented

dx.doi.org/10.1021/jm301422h | J. Med. Chem. XXXX, XXX, XXX–XXX

toward the outer part of the molecule and therefore more accessible to interactions with the surroundings. In the bridged analogue, the nitrogen lone pair is only partially available. Because of steric hindrance, this lone pair is buried in the structure and unavailable for interaction with solvents or other molecules. From the MEP surface of the corresponding 4-aminoquinoline fragment **3b**, two more electronegative sites can be observed. As expected, the primary terminal amino group that is unavailable in **5b** and partly available in **4b** is completely available in **3b**, displaying an increased electronegative surface. The most interesting difference stems from the electronegatively charged zone of the nitrogen of the 4-position in the quinoline ring. Absent in both ferrocenyl derivatives, the electron density associated with this nitrogen is thought to be affected by the inductive and electronic changes generated by the attachment of the ferrocene. When compared to the MEP surface of ferroquine, the principal difference noticed with both types of ferrocene derivatives, series **5** and series **4**, is the availability of the alkyl nitrogen. The conformation and the electrostatic distribution of charge in ferroquine appear to be similar to those observed in series **5**, with the electron density of the tertiary nitrogen partially available and hidden in a pocket of the structure. Ferrocenyl derivatives in general, compared to the organic 4-aminoquinoline fragment, have a reduced negative charged surface area due to a hindered alkyl nitrogen and at the nitrogen at the 4-position in the quinoline ring.

The polar surface area (PSA) along with the partition coefficients can estimate successfully the capability of compounds to permeate cell membranes, and this is strictly related to an increased accumulation in the cellular organelle.[62,63] The topological polar surface area (PSA) of a molecule is a measure of the surface rich in oxygen or nitrogen atoms, or hydrogen atoms attached to nitrogen or oxygen atoms, and serves as an indication of how heavily hydrated it will be in an aqueous environment.[64] This parameter estimates the H-bonding ability of a molecule and provides good correlation with experimental transport data, making it an attractive potential predictor of membrane transport.[65] During the absorption process, a compound must be able to shed its hydration sphere to enter the lipophilic membrane environment. If the compound is heavily solvated, this process is likely to be energetically unfavorable, and so absorption will be hindered.[64] Consequently, compounds with lower PSA values, less than 60−140 Å^2, are good at permeating cell membranes.[62,64,66] PSA values for a selection of compounds in their neutral state are presented in Table 6. All studied compounds have PSA of less than 60−140 Å^2 cutoff. All the bridged ferrocenyl compounds seem to have similar relatively low values of PSA ranging from 22 to 27 Å^2. The monosubstituted ferrocenyl compounds **4a−e** display higher PSA values, likely stemming from the alkyl nitrogen availability observable in their MEP surfaces (Figure 5). The corresponding quinoline analogues **3a−e**, as expected, have even higher PSA values, almost double those registered for the bridged ferrocenyl group. This is explained by the additional electronic surface (Figure 5). Interestingly, the PSA value of ferroquine (FQ) falls in the range of values obtained for the bridged ferrocenyl compounds **5**, confirming the similarity observed in the map of electrostatic potential of these compounds. Although the PSA value is not the only parameter to consider, it indicates that ferroquine and the bridged ferrocenyl compounds should have similar permeability/absorption profiles.

Structure−Activity Relationship. Structural features play a remarkable role in the interaction of these compounds with the parasite transmembrane proteins that allow the accumulation of the drug inside the parasite food vacuole, influence its ability to accumulate in the vacuole, and therefore overcome drug resistance. The following discussion encompasses a correlation of each physical property discussed previously with the antiplasmodial activity observed mainly against the chloroquine-sensitive strain D10 and the chloroquine-resistant strain Dd2.

Antiplasmodial Activity, Hydrogen Bonding and Conformation. The presence of intramolecular hydrogen bonding has been associated with the improved action of ferroquine.[17,21] It is believed that intramolecular hydrogen bonding will give rise to a closed conformation that can penetrate more efficiently the parasite membranes to reach the drug site of action.[17] Intramolecular hydrogen bonding between the aromatic NH on the 4-position of the quinoline ring and the nitrogen atom in the β-position of the cyclopentadienyl ring of ferrocene was observed in a low dielectric constant solvent (chloroform) by the means of ^{1}H NMR spectroscopy. All compounds that exhibited shifts in the ^{1}H−N$_{Ar}$ NMR signals toward higher frequencies (indicating the deshielding effect of the formation of intramolecular hydrogen bonding) also exhibited reasonable antiplasmodial activity. The exception of the group is compound **4e**, the 2,2′-dimethylpropylalkyl chain derivative that, despite the most pronounced positive shifting, is inactive, especially in the chloroquine-resistant strain Dd2. Compounds that suffered shifts in the ^{1}H−N$_{Ar}$ NMR signals toward lower frequencies (indicating weakening/loss of hydrogen bonding, likely due to conformational restrictions) had mixed results in terms of antiplasmodial activity. Compound **5c**, with a relatively small shifting to lower frequencies, is one of the most active of the group; however, **5b** and **5e**, which shifted −1.68 and −3.35 ppm, respectively, were among the least active. These observations confirm that the intramolecular H-bonding observed in solution is associated, with certain exceptions, with an increase in antiplasmodial activity and that the opposite is also true, loss of intramolecular H-bonding interaction is associated with decrease of antiplasmodial action. This correlation is illustrated in Figure 6. Intramolecular hydrogen bonding was also observed in the solid state. Compound **4e**, one of the least active compounds, presents intramolecular H-bonding, while **4b** and **5b** that surpass its antiplasmodial activity against both parasite strains lack this bonding in the solid state. These observations agree with our previous observations that the branching of the side chain is a bigger influence than intramolecular H-bonding when determining antiplasmodial activity.

It has been suggested that a *N*-quinoline to *N*-methylene chain distance in the range of 7.52−10.21 Å is required for the formation of a heme−drug complex and therefore for antiplasmodial activity.[26] The corresponding distances are 8.912, 6.685, and 7.653 Å in compounds **4b**, **4e**, and **5b**, respectively. It is worth noting that the only compound in this group that does not follow this rule is the least active of the three (**4e**) and one of the least active compounds of the complete group. The intramolecular H-bonding and the conformation observed in the solid state structure of **4e** are similar to those of ferroquine with the quinoline ring found on top of the ferrocene skeleton.[17] Nonetheless, their antiplasmodial activities are remarkably different. The conformation of **5b** (Figure 1) is unusual in ferrocenyl quinoline antimalarials, with the quinoline ring parallel to the ferrocene skeleton but in two distinct planes.

dx.doi.org/10.1021/jm301422h | J. Med. Chem. XXXX, XXX, XXX−XXX

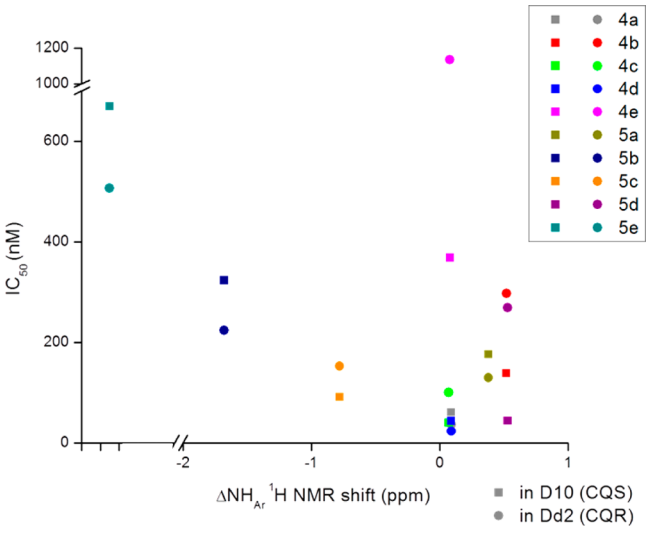

Figure 6. ^{1}H NMR spectroscopic shift of the $^{1}H-N_{Ar}$ (as indicator of formation/loss of intramolecular hydrogen bond) vs the in vitro antiplasmodial activity against *P. falciparum* CQS D10 and CQR Dd2 parasite strains. The most active compounds (low IC_{50}) fall to the right of the diagram corresponding to the shifting of the $^{1}H-N_{Ar}$ hydrogen toward higher frequencies (forming of hydrogen bond).

These conformational characteristics, observed in chloroform and in the solid state, are likely to remain similar in the presence of low dielectric media such as the lipid environment where these compounds accumulate and act.

Monosubstituted derivatization with ferrocene (such in **4a−e**) seems to increase the formation of intramolecular H-bonding. On the contrary, formation of the bridged ferrocenyl compounds (such in **5a−e**) seems to cause the loss of the intramolecular H-bond, likely due to conformational restrictions exerted by the bridge structure. The presence of an intramolecular H-bond is generally associated with the increase of antiplasmodial action, and in turn, the loss of this bonding seems to decrease the action. However, the exceptions to this rule point out that other factors might have a bigger influence in determining the activity. This would suggest that H-bonding is relevant but not determinant for antiplasmodial activity.

Antiplasmodial Activity, Hematin Association, and *β*-Hematin Formation Inhibition. All compounds exhibited interaction with Fe(III)PPIX. The trend observed was the decrease of association constants (expressed as log *K*) from the purely organic fragments series **3** to the ferrocenyl derivatives, both series **4** and **5**, regardless of length or branching of the methylene side chain. In general, large association constants were observed in compounds that were the most active, although the opposite was not observed, as is the case of **4d** and **5a** that, with the lowest found values of association constants, log *K* = 3.68 and 4.18, respectively, were among the most active compounds tested. The association constants and the antiplasmodial activity against the chloroquine-resistant Dd2 parasite strain show no clear correlation. This supports the notion that while association with hematin is important, a more important process is the delivery of relevant amounts of the drug to the site of action through the crossing of membranes. Unfortunately, solubility requirements made it impossible to prove the *β*-hematin inhibition property of these compounds.

Antiplasmodial Activity, Lipophilicity, and Hydrophilicity. The influence of the ferrocene in the overall balance between lipophilicity and hydrophilicity of the molecule was explored by examining the calculated lipophilicity with the PSA values and the antiplasmodial activity observed. This is likely to be relevant in determining the accumulation of the ferrocenyl drug, considering that the drug must cross a number of membranes to reach the inner part of the parasite food vacuole. When the partition coefficient (log *P*) values are correlated to their antiplasmodial action in the chloroquine-sensitive D10 strain, the increase of lipophilicity is detrimental, since all ferrocene derivatives are less active than their corresponding organic components. Much more interesting is the correlation observed in the chloroquine-resistant parasite strains. In the organic series **3a−e**, an increase in lipophilicity helped to improve the antiplasmodial action, with the most active compound being **3e**. In the case of the monosubstituted ferrocenyl compounds **4a−e**, the increase in lipophilicity due to the ferrocene produced a 4- to 15-fold improvement in the activity for compounds **4a−d**. For compound **4e**, the most lipophilic of the group (ClogP = 5.64), a significant decrease in activity is observed. Finally, in the case of the bridged ferrocenyl compounds **5a−e**, the closed conformation represents an even greater increase in lipophilicity compared to series **4**. This is reflected in a decrease in the antiplasmodial activity of the first four compounds. Thus, an increase in lipophilicity was beneficial in improving the activity of the compounds against drug-resistant strains but only to a certain level. When the compounds become too lipophilic, antiplasmodial activity decreases, as can be appreciated in Figure 7. This would

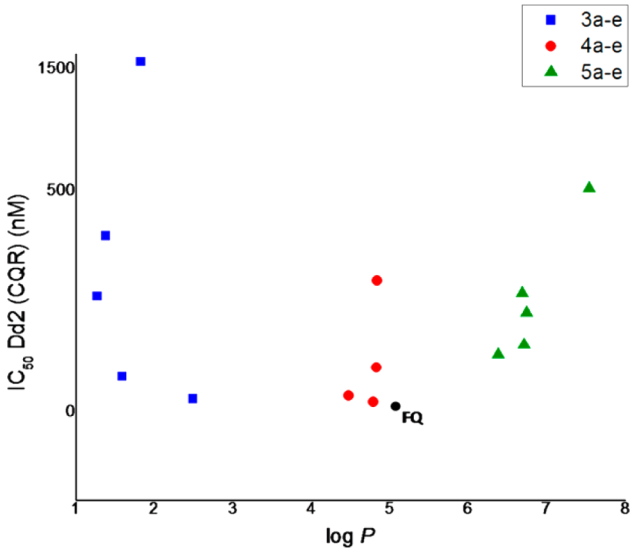

Figure 7. Theoretically calculated partition coefficients (ClogP) vs the in vitro antiplasmodial activity against *P. falciparum* CQR Dd2 parasite strain. The most active compounds (low IC_{50}) present partition coefficients in the range of ClogP = 4.5−5.0.

explain the reduced activity observed for the 2,2′-dimethylpropylferrocenyl derivatives. The better activity observed for **5e** (vs **4e**) could be explained by its more closed conformation that possibly aids in its transportation across membranes with its reduced surface. Indeed, an intermediate lipophilicity that delivers the best activity seems to be in the range of ClogP = 4.5−5.1, which is coincidentally where the lipophilicity of ferroquine falls (log *P* = 5.1).

The hydrophilicity of these compounds was studied by means of molecular electrostatic potential (MEP) surfaces and

dx.doi.org/10.1021/jm301422h | J. Med. Chem. XXXX, XXX, XXX−XXX

polar surface values (PSA). The bridged compounds **5a−e** presented MEP surfaces of reduced electronegatively charged area. The lone pair of the methylene nitrogen is described as buried in the structure and mostly inaccessible for interaction with solvents or other molecules and less prone to participate in solvation. Interestingly, the two compounds that showed partial availability of the electronic cloud associated with this nitrogen, **5a** and **5c**, were also the most potent compounds of this series and those resembling most the MEP surface obtained for ferroquine. Compounds of the series **4a−e** and **3a−e** have increased electrostatic potential surface. While this improved the antiplasmodial action in most but not in all of the compounds of series **4**, the further increase in electronegatively charged area in the purely organic derivatives series **3** decreases the antiplasmodial effectiveness against the drug-resistant strain. These observations are consistent with the values observed for the polar surface area (PSA). The bridged compounds **5a−e** have relatively low values of PSA, from 21 to 27 Å^2. The most active compound of this series, **5c**, has a PSA value of 26.0 Å^2, very similar to that of ferroquine, 26.2 Å^2. Compound **5e** has, as expected, the lowest value of PSA, but that is also accompanied by relatively low activity. Higher PSA values for **3b** and **4b** are correlated to lower activity. Therefore, it seems that more than a trend, a balance, must be reached where the amount of electronegative surface is slightly more than that observed for the bridged compounds series **5** but not as much as that observed for compounds series **4**, much like what is observed for ferroquine. The ideal hydrophilicity that delivers the best activity seems to be in the approximate range of PSA = 25.9−26.2 Å^2. Even more illustrative is the correlation between the resistance index (RI) and PSA values shown in Figure 8. PSA

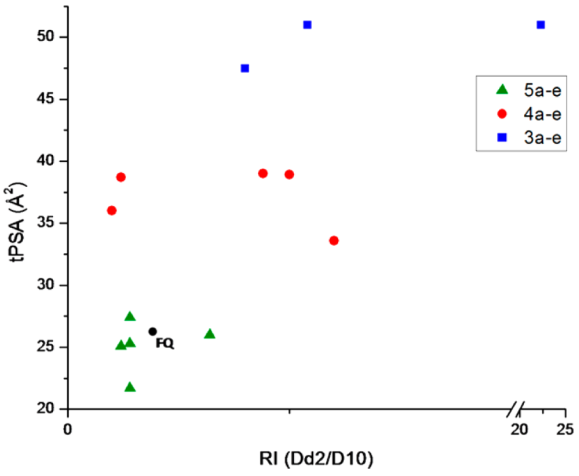

Figure 8. Resistance index (RI, IC_{50}(CQR Dd2)/IC_{50}(CQS D10)) vs the topological polar surface area (tPSA) values. The compounds that demonstrated the best capacity to avoid resistance development (RI close to 1) present tPSA values in the range 25.0−28.0 Å^2. Points corresponding to **3a** (RI = 7.3) and **3b** (RI = 7.8) are not visible because of the break in the *x* axis.

values in the range 25.9−26.2 Å^2 seem to confer lower resistance indices, suggesting that this physical property is determinant for the overcoming of resistance mechanisms.

It is hypothesized that the closed conformation observed in compounds **5a−e**, which resemble ferroquine, gives the compounds a close to ideal balance where the very lipophilic ferrocene is sticking to the side but parallel to the quinoline ring without disturbing its interaction with hematin. The hydrophobic ferrocene can then establish favorable van der Waals interactions with lipid surfaces at the interface with the membranes to be crossed and aid in the accumulation of the drug. This particular conformation, its compact size, and lipophilicity/hydrophilicity balance could provide these compounds with the structural characteristics needed to escape the resistance mechanism of the transmembrane proteins and achieve significant accumulation inside the parasite food vacuole. This would explain why their activity is increased in drug-resistant strains.

CONCLUSION

Five disubstituted ferrocene chloroquine derivatives with the terminal nitrogen of the chloroquine derivative bridging the two cyclopentadienyl rings of ferrocene (**5a−e**) were synthesized and structurally compared to the corresponding monosubstituted ferrocene chloroquine (**4a−e**) analogues and to the corresponding organic fragments (**3a−e**). All compounds were characterized by a variety of physical methods. The presence or absence of hydrogen bonding interactions, the conformation, the degree of rigidity, and the lipophilicity of these derivatives are correlated to the biological responses of these compounds against different strains of *P. falciparum* parasites. All compounds were active against both chloroquine-sensitive and resistant parasite strains. Bridged disubstituted ferrocenyl compounds **5a−e** were able to overcome resistance and, in all cases except one (**5e**), were more active in the resistant strain than in the sensitive one, giving them appealing resistance indices of <1. The branching of the methylene spacer was found to be a strong influence in activity, with the derivatives losing efficacy as they grow in branching. The length of this spacer was not a strong influence. The presence of an intramolecular H-bond is relevant but not determinant for antiplasmodial activity. Association with hematin was observed for all compounds and did not seem to determine the activity in vitro. A balance between the lipophilicity and the hydrophilicity was found to be determinant in the activity displayed by the compounds. The addition of the ferrocenyl unit contributed largely to increase the lipophilicity of the compound, and that has been related in the past to improved transport of the drug through membranes.[17] It was found that log *P* values of 4.5−5.0 and PSA values of ∼26.0 Å^2 give the best balance, and that is witnessed in the increase of activity. The values found for both parameters happen to be consistent with what is observed in ferroquine.

Thus, compounds **5** would benefit from being slightly more hydrophilic with more electronegative area available and from having an intramolecular hydrogen-bonding interaction that could allow the "flip-flop" mechanism that has been postulated for aiding in the accumulation of ferroquine when crossing membranes. With these characteristics in mind and with the parameters observed to be determinant in antiplasmodial activity, in silico calculation could aid in the design of more ferroquine analogues with tuned lipophilicity/hydrophilicity and intramolecular hydrogen bonding, giving analogues more potent than ferroquine.

EXPERIMENTAL SECTION

Materials and Instrumentation. All syntheses were performed using dried solvents under an inert atmosphere (nitrogen or argon) using Schlenk-type glassware unless otherwise indicated. Solvents were dried and distilled prior to use. All other chemicals were purchased

dx.doi.org/10.1021/jm301422h | J. Med. Chem. XXXX, XXX, XXX−XXX

from Sigma Aldrich or Acros Organics and used without further purification. Selected syntheses were carried using a microwave reactor Initiator 2.5 (Biotage). The products were purified to >95% and were confirmed by HPLC (using linear gradient of 100% water to 100% acetonitrile) and/or elemental analysis. Column chromatography was performed using UltraPure silica gel (230−400 mesh) (SiliCycle) or alumina neutral (60−325 mesh) (Fisher Scientific). An automated column system CombiFlashRf (Teledyne ISCO, Inc.) was also employed using RediSepRf gold silica high performance columns. ^{1}H and ^{13}C NMR spectra were recorded at room temperature on Bruker AV-300, AV-400dir, AV-400inv, and AV-600 instruments. The NMR spectra are expressed on the δ (ppm) scale and referenced to residual solvent peaks or internal tetramethylsilane. The NMR assignments were supported by additional 2D experiments (^{1}H−^{1}H COSY, ^{1}H−^{13}C HSQC, ^{1}H−^{13}C HMBC). High resolution mass spectrometry and elemental analyses were performed at the UBC Chemistry Mass Spectrometry and Microanalysis Services. Low resolution mass spectra were obtained using a Bruker Esquire ion trap ESI-MS spectrometer. High resolution mass spectra were obtained on a Waters/Micromass LCT spectrometer. Elemental analyses were performed on a Carlo Erba elemental analyzer EA 1108. Semipreparative high-performance liquid chromatography (HPLC) was performed on a system outfitted with a Waters W600 solvent gradient controller and a Waters 2487 dual wavelength absorbance detector set, and a XTerraRP column (187 μm, 19 mm × 300 mm) was used. Solvent flow rate was 10 mL/min with a 25 min gradient from 100% H_2O (0.1% trifluoroacetic acid, TFA) to 100% CH_3CN. X-ray data were collected and processed using a Bruker X8 APEX II diffractometer with graphite monochromated Mo Kα radiation. The structures were solved using the Bruker SAINT software package (SAINT, version 7.60A, Bruker AXS Inc., Madison, WI, U.S., 1997−2009). All non-hydrogen atoms were refined anisotropically. All hydrogen atoms were placed in calculated positions. All N−H hydrogen atoms were located in difference maps and refined isotropically. All other hydrogen atoms were included in calculated positions but not refined. Further crystal structure exploration and analysis were conducted using the Mercury software package (version.2.3, CCDC, Cambridge, U.K.).

1,1′-Bis(*N*,*N*′-dimethylaminomethyl)ferrocene (1). This compound was prepared as previously reported[67] with slight modifications. *n*-Butyllithium (1.6 M in hexanes, 32.8 mL, 52.5 mmol, 2.1 equiv) was added dropwise to a stirred solution of freshly distilled TMEDA (7.83 mL, 52.5 mmol, 2.1 equiv) in hexanes (10 mL). Ferrocene (4.65 g, 25.0 mmol, 1.0 equiv) was dissolved in hexanes (180 mL) and added dropwise by syringe over 1 h. The reaction mixture was stirred under inert atmosphere at room temperature for 12 h. The solution was further diluted with THF (200 mL), and (*N*,*N*′-dimethyl)methyleneammonium iodide (9.7 g, 52.5 mmol, 2.1 equiv) was added in one portion. The reaction mixture was heated under reflux for 10 min and then allowed to cool to room temperature and stirred under inert atmosphere for 24 h. Water (30 mL) was added to terminate the reaction. The organic layer was separated, and the aqueous layer was extracted with portions of diethyl ether (3 × 25 mL). The combined organic fractions were dried over anhydrous $MgSO_4$ and the solvent was removed under reduced pressure to afford an orange-brown oil. Purification of the desired product was done by flash column chromatography on neutral alumina Brockman activity V. Elution was achieved with petroleum ether to obtain unreacted ferrocene, with diethyl ether/petroleum ether (3:7) to obtain the monodimethylaminomethyl derivative, and with methanol/diethyl ether (3:97) to obtain product **1** as an orange-brown oil (2.64 g, 8.79 mmol, 35%). ^{1}H NMR (400 MHz, $CDCl_3$): δ (ppm) 4.10 (t, ^{3}J = 1.71 Hz, 4H), 4.07 (t, ^{3}J = 1.71 Hz, 4H), 3.27 (s, 4H), 2.17 (s, 12H).

1,1′-Bis(*N*,*N*′-trimethylaminomethyl)ferrocene iodide (2). On the basis of a previously published method,[67] iodomethane (1.4 mL, 22.4 mmol, 3 equiv) was added slowly to a solution of 1,1′-bis(*N*,*N*-dimethylaminomethyl)ferrocene (**1**, 2.24 g, 7.47 mmol, 1 equiv) in methanol (40 mL) under inert atmosphere. The resulting solution was heated at reflux for 10 min before cooling to room temperature. Diethyl ether (150 mL) was then added and the product precipitated as a pale yellow solid, which was collected by filtration, washed with dichloromethane (30 mL), and diethyl ether (2 × 25 mL) before being dried under vacuum to yield 1,1′-bis(*N*,*N*′-trimethylaminomethyl)-ferrocene iodide **2** as a yellow powder (3.0 g, 6.2 mmol, 83%). ^{1}H NMR (300 MHz, CD_3OD): δ (ppm) 4.69 (s, 4H), 4.66 (t, ^{3}J = 1.83 Hz, 4H), 4.56 (t, ^{3}J = 1.96 Hz, 4H), 3.07 (s, 18H). ESI-MS(+): 457.1 $[M - I^-]^+$. Anal. Calcd for $C_{18}H_{30}FeI_2N_2$: C, 37.01; H, 5.18; N, 4.08. Found: C, 37.34; H, 5.13; N, 4.58.

General Procedure for the Synthesis of 4-Aminoquinoline Derivatives (3a−e). *N*-(7-Chloroquinolin-4-yl)ethane-1,2-diamine (**3a**), *N*-(7-chloroquinolin-4-yl)propane-1,3-diamine (**3b**), *N*-(7-chloroquinolin-4-yl)butane-1,4-diamine (**3c**), *N*-(7-chloroquinolin-4-yl)-propane-1,2-diamine (**3d**), and *N*-(7-chloroquinolin-4-yl)-2,2-dimethylpropane-1,3-diamine (**3e**) were prepared by following modifications from literature procedures.[7,30,32,68] 4,7-Dichloroquinoline (1 g, 5.04 mmol, 1 equiv) was dissolved in the respective diamine (approximately 50.4 mmol, 10 equiv) in a 20 mL microwave vial. The mixture was heated using a heat gun until complete dissolution. The reaction was carried out in a microwave reactor for 30 min at 165 °C. After the vial was cooled to room temperature, aqueous NaOH (1 N, 10 mL) was added and the mixture was extracted with methylene chloride (3 × 15 mL). The organic fractions were combined and successively washed with water (3 × 10 mL) and brine (3 × 10 mL). The organic layer was dried over anhydrous $MgSO_4$, and the solvent was removed under reduced pressure. The respective products (**3a−e**) were obtained by precipitation after the addition of a 8:2 hexane/methylene chloride solution.

***N*-(7-Chloroquinolin-4-yl)ethane-1,2-diamine (3a).** This compound was obtained as a yellow solid (0.74 g, 3.33 mmol, 65%). ^{1}H NMR (300 MHz, $CDCl_3$): δ (ppm) 8.52 (d, ^{3}J = 5.5 Hz, 1H), 7.95 (d, ^{4}J = 2.1 Hz, 1H), 7.74 (d, ^{3}J = 9.1 Hz, 1H), 7.35 (dd, ^{3}J = 9.1 Hz, ^{4}J = 2.1 Hz, 1H), 6.40 (d, ^{3}J = 5.5 Hz, 1H), 5.82 (br s, 1H), 3.32 (m, 2H), 3.12 (m, 2H), 1.48 (br s, 2H). ^{13}C NMR (75 MHz, $CDCl_3$): δ (ppm) 152.2, 150.1, 149.3, 135.0, 128.9, 125.4, 121.4, 117.6, 99.4, 44.9, 40.4. IR (ATR): ν 3247 (broad), 2894 (w), 2852 (w), 1582 (s), 1541 (s), 1454 (m), 1426 (m), 1340 (m), 1325 (m), 1163 (w), 1141 (w), 1020 (w), 867 (m), 800 (s), 758 (m) [cm^{-1}]. Anal. Calcd for $C_{11}H_{12}ClN_3$: C, 59.60, H, 5.46, N, 18.95. Found: C, 59.34, H, 5.42, N, 18.87. ESI-MS (HR) calculated for $C_{11}H_{13}ClN_3^+$: 222.0798. Found: 222.0793 $[M + H]^+$.

***N*-(7-Chloroquinolin-4-yl)propane-1,3-diamine (3b).** This compound was obtained as a beige solid (1.08 g, 4.55 mmol, 89%). ^{1}H NMR (300 MHz, $CDCl_3$): δ (ppm) 8.50 (d, ^{3}J = 5.3 Hz, 1H), 7.93 (d, ^{4}J = 1.9 Hz, 1H), 7.72 (d, ^{3}J = 9.0 Hz, 1H), 7.44 (br s, 1H), 7.31 (dd, ^{3}J = 9.0 Hz, ^{4}J = 1.9 Hz, 1H), 6.33 (d, ^{3}J = 5.3 Hz, 1H), 3.42 (m, 2H), 2.87 (t, ^{3}J = 5.7 Hz, 2H), 1.90 (m, ^{3}J = 5.7 Hz, 2H), 1.65 (br s, 2H). ^{13}C NMR (75 MHz, $CDCl_3$): δ (ppm) 152.3, 150.6, 149.4, 134.8, 128.7, 125.1, 122.2, 117.7, 98.4, 43.9, 41.7, 30.1. IR (ATR): ν 3255 (broad), 2934 (w), 2866 (w), 2238 (w), 1580 (s), 1542 (m), 1474 (w), 1434 (m), 1371 (m), 1331 (m), 1284 (m), 1202 (w), 1137 (m), 1078 (w), 899 (s), 851 (s), 800 (s), 818 (m), 763 (s) [cm^{-1}]. ESI-MS (HR) calculated for $C_{12}H_{15}ClN_3^+$: 236.0955. Found: 236.0953 $[M + H]^+$.

***N*-(7-Chloroquinolin-4-yl)butane-1,4-diamine (3c).** This compound was obtained as an off-white solid (0.62 g, 2.48 mmol, 48%). ^{1}H NMR (400 MHz, $CDCl_3$): δ (ppm) 8.53 (d,^{3}J = 5.5 Hz, 1H), 7.95 (d, ^{4}J = 2.1 Hz, 1H), 7.74 (d, ^{3}J = 8.8 Hz, 1H), 7.34 (dd, ^{3}J = 8.8, ^{4}J = 2.1 Hz, 1H), 6.39 (d, ^{3}J = 5.5 Hz, 1H), 6.00 (br s, 1H), 3.32 (m, 2H), 2.84 (t, ^{3}J = 6.5 Hz, 2H), 1.88 (quin, ^{3}J = 6.9 Hz, 2H), 1.67 (quin, ^{3}J = 6.9 Hz, 2H), 1.44 (br s, 2H). ^{13}C NMR (101 MHz, $CDCl_3$): δ (ppm) 152.1, 149.2, 144.1, 134.7, 128.8, 125.0, 121.4, 117.3, 98.8, 43.2, 41.5, 30.8, 26.1. IR (ATR): ν 3247 (broad), 2930 (w), 2858 (w), 1576 (s), 1540 (m), 1449 (m), 1431 (m), 1368 (s), 1331 (m), 1284 (w), 1252 (m), 1198 (w), 1130 (m), 972 (w), 898 (s), 849 (s), 817 (m), 794 (s), 766 (s) [cm^{-1}]. ESI-MS (HR) calculated for $C_{13}H_{17}ClN_3^+$: 250.1111. Found: 250.1114 $[M + H]^+$.

***N*-(7-Chloroquinolin-4-yl)propane-1,2-diamine (3d).** This compound was obtained as an off-white solid (0.68 g, 2.88 mmol, 56%). ^{1}H NMR (400 MHz, $CDCl_3$): δ (ppm) 8.53 (d, ^{3}J = 5.5 Hz, 1H), 7.96 (d, ^{4}J = 2.0 Hz, 1H), 7.75 (d, ^{3}J = 8.9 Hz, 1H), 7.38 (dd, ^{3}J = 8.9 Hz, ^{4}J = 2.0 Hz, 1H), 6.40 (d, ^{3}J = 5.5 Hz, 1H), 5.85 (br s, 1H), 3.32 (m, 2H), 3.00 (m, 1H), 1.64 (s, 2H), 1.27 (d, ^{3}J = 6.1 Hz, 3H).

dx.doi.org/10.1021/jm301422h | J. Med. Chem. XXXX, XXX, XXX−XXX

^{13}C NMR (101 MHz, $CDCl_3$): δ (ppm) 152.4, 150.2, 149.5, 135.1, 129.1, 125.6, 121.5, 117.7, 99.5, 50.3, 46.1, 23.3. IR (ATR): ν 3258 (broad), 3010 (w), 2962 (w), 1576 (s), 1538 (m), 1490 (w), 1451 (m), 1368 (m), 1334 (m), 1312 (w), 1282 (w), 1254 (w), 1198 (w), 1135 (m), 1085 (w), 1014 (w), 959 (m), 919 (s), 901 (s), 846 (s), 794 (s), 765 (m) [cm^{-1}]. Anal. Calcd for $C_{12}H_{14}ClN_3$: C, 61.15, H, 5.99, N, 17.83. Found: C, 61.22, H, 5.96, N, 17.76. ESI-MS (HR) calculated for $C_{12}H_{15}ClN_3^+$: 236.0955. Found: 236.0948 $[M + H]^+$.

***N*-(7-Chloroquinolin-4-yl)-2,2-dimethylpropane-1,3-diamine (3e).** This compound was obtained as a yellowish solid (0.70 g, 2.62 mmol, 52%). ^{1}H NMR (300 MHz, $CDCl_3$): δ (ppm) 8.48 (br s, 1H), 8.47 (d, ^3J = 5.4 Hz, 1H), 7.91 (d, ^4J = 2.2 Hz, 1H), 7.72 (d, ^3J = 9.0 Hz, 1H), 7.29 (dd, ^3J = 9.0 Hz, ^4J = 2.2 Hz, 1H), 6.27 (d, ^3J = 5.4 Hz, 1H), 3.18 (br s, 2H), 2.87 (br s, 2H), 1.68 (br s, 2H), 1.08 (s, 6H). ^{13}C NMR (75 MHz, $CDCl_3$): δ (ppm) 152.3, 151.1, 149.4, 134.7, 128.6, 124.9, 122.5, 117.9, 98.0, 55.9, 52.9, 34.0, 24.7. IR (ATR): ν 3169 (broad), 2959 (w), 2839 (w), 1579 (s), 1541 (m), 1448 (m), 1429 (m), 1364 (m), 1312 (m), 1277 (m), 1246 (w), 1202 (m), 1138 (m), 1073 (w), 899 (m), 872 (m), 848 (m), 793 (m), 764 (m), 675 (m), 638 (s) [cm^{-1}]. Anal. Calcd for $C_{14}H_{18}ClN_3$: C, 63.75, H, 6.88, N, 15.93. Found: C, 63.16, H, 6.83, N, 15.85. ESI-MS (HR) calculated for $C_{14}H_{19}ClN_3^+$: 264.1268. Found: 264.1270 $[M + H]^+$.

General Procedure for the Synthesis of Monosubstituted Ferrocenyl 4-Aminoquinoline Derivatives (4a–e). These compounds were prepared as previously reported (with the exception of **4d**)[7] with modifications. Ferrocenecarboxaldehyde (0.214 g, 1.0 mmol, 1 equiv) and the corresponding 4-aminoquinoline derivatives **3a–e** (1.10 mmol, 1.1 equiv) were dissolved in dry methanol (20 mL). The mixture was stirred at room temperature overnight. Sodium borohydride (0.114 g, 3.0 mmol, 3 equiv) was added, and the resulting mixture was stirred for an additional 2 h. The reaction mixture was quenched with the addition of 5% $NaHCO_3$ solution (10 mL), and the resulting mixture was extracted with diethyl ether (3 × 20 mL). The combined organic fractions were dried over anhydrous Na_2SO_4, and solvent was removed under reduced pressure. Purification of the desired product was done by flash column chromatography on silica with a mixture of ethyl acetate/methanol/TEA in increasing polarity, 94:4:2 to 75:15:10 ratios.

***N*-(7-Chloro-4-quinolyl)-*N*′-ferrocenyl-ethane-1,2-diamine (4a).** This product was obtained as an orange solid (0.254 g, 0.61 mmol, 61%). ^{1}H NMR (300 MHz, $CDCl_3$): δ (ppm) 8.52 (d, ^3J = 5.4 Hz, 1H, 9-H), 7.95 (d, ^4J = 2.1 Hz, 1H, 11-H), 7.70 (d, ^3J = 8.9 Hz, 1H, 14-H), 7.35 (dd, ^3J = 8.9 Hz, ^4J = 2.1 Hz, 1H, 13-H), 6.38 (d, ^3J = 5.4 Hz, 1H, 8-H), 5.91 (br, 1H, Ar-N*H*-), 4.19 (m, 2H, 2-H), 4.14 (m, 2H, 3-H), 4.13 (s, 5H, Cp-H), 3.59 (s, 2H, 4-H), 3.31 (m, 2H, 6-H), 3.05 (m, 2H, 5-H), 1.92 (vb, 1H, CH_2NHCH_2). ^{13}C NMR (75 MHz, $CDCl_3$): δ (ppm) 152.3 (C9), 150.1 (C7), 149.3 (C10), 135.0 (C12), 128.8 (C11), 125.4 (C13), 121.6 (C14), 117.6 (C15), 99.4 (C8), 86.5 (C1), 68.7 (*Cp*), 68.6 (C2), 68.2 (C3), 48.5 (C4), 47.0 (C6), 42.1 (C5). IR (ATR): ν 3245 (broad), 3083 (w), 2924 (w), 2851 (w), 1577 (s), 1532 (m), 1449 (m), 1367 (m), 1328 (m), 1277 (w), 1231 (w), 1138 (w), 1104 (m), 1079 (w), 1023 (w), 999 (m), 803 (s), 765 (m), 642 (m) [cm^{-1}]. Anal. Calcd for $C_{22}H_{22}ClFeN_3$: C, 62.95, H, 5.28, N, 10.01. Found: C, 62.72, H, 5.38, N, 9.82. ESI-MS (HR) calculated for $C_{22}H_{23}ClFeN_3^+$: 420.0930. Found: 420.0931 $[M + H]^+$.

***N*-(7-Chloro-4-quinolyl)-*N*′-ferrocenyl-propane-1,3-diamine (4b).** This product was obtained as a yellow solid (0.356 g, 0.82 mmol, 82%). ^{1}H NMR (300 MHz, $CDCl_3$): δ (ppm) 8.50 (d, ^3J = 5.4 Hz, 1H, 10-H), 7.96 (br, 1H, Ar-N*H*-), 7.93 (d, ^4J = 2.0 Hz, 1H, 12-H), 7.62 (d, ^3J = 8.9 Hz, 1H, 15-H), 7.27 (dd, ^3J = 8.9 Hz, ^4J = 2.0 Hz, 1H, 14-H), 6.29 (d, ^3J = 5.4 Hz, 1H, 9-H), 4.24 (m, 2H, 2-H), 4.22 (m, 2H, 3-H), 4.17 (s, 5H, Cp-H), 3.62 (s, 2H, 4-H), 3.38 (m, 2H, 7-H), 2.98 (m, 2H, 5-H), 1.92 (m, 2H, 6-H), 1.80 (vb, 1H, CH_2NHCH_2). ^{13}C NMR (75 MHz, $CDCl_3$): δ (ppm) 152.4 (C10), 150.8 (C8), 149.4 (C11), 134.7 (C13), 128.7 (C12), 125.1 (C14), 122.7 (C15), 117.8 (C16), 98.3 (C9), 86.0 (C1), 68.9 (C2), 68.7 (Cp), 68.4 (C3), 49.8 (C4), 49.7 (C7), 44.5 (C5), 27.4 (C6). IR (ATR): ν 3198 (w), 3088 (w), 2945 (w), 2826 (w), 1578 (s), 1539 (m), 1490 (w), 1445 (m), 1432 (m), 1364 (m), 1327 (m), 1283 (m), 1240 (m), 1139 (m), 1102 (m), 1056 (w), 1000 (m), 899 (w), 854 (m), 817 (s), 801 (s), 767 (m), 643 (m), 620 (m) [cm^{-1}]. Anal. Calcd for $C_{23}H_{24}ClFeN_3$: C, 63.69, H, 5.58, N, 9.69. Found: C, 63.67, H, 5.59, N, 9.62. ESI-MS (HR) calculated for $C_{23}H_{25}ClFeN_3^+$: 434.1086. Found: 434.1089 $[M + H]^+$.

***N*-(7-Chloro-4-quinolyl)-*N*′-ferrocenyl-butane-1,4-diamine (4c).** This product was obtained as a light yellow solid (0.323 g, 0.72 mmol, 72%). ^{1}H NMR (300 MHz, $CDCl_3$): δ (ppm) 8.52 (d, ^3J = 5.5 Hz, 1H, 11-H), 7.95 (d, ^4J = 2.1 Hz, 1H, 13-H), 7.74 (d, ^3J = 8.9 Hz, 1H, 16-H), 7.31 (dd, ^3J = 8.9 Hz, ^4J = 2.1 Hz, 1H, 15-H), 6.37 (d, ^3J = 5.5 Hz, 1H, 10-H), 6.07 (br, 1H, Ar-N*H*-), 4.20 (d, ^3J = 1.8 Hz, 2H, 2,3-H), 4.14 (s, 5H, Cp-H), 3.59 (s, 2H, 4-H), 3.30 (m, 2H, 8-H), 2.76 (m, 2H, 5-H), 2.32 (br s, 1H, CH_2NHCH_2), 1.86 (m, 2H, 7-H), 1.72 (m, 2H, 6-H). ^{13}C NMR (75 MHz, $CDCl_3$): δ (ppm) 155.5 (C11), 155.1 (C9), 151.9 (C12), 134.8 (C14), 128.5 (C13), 125.1 (C15), 121.6 (C16), 117.3 (C17), 98.8 (C10), 85.3 (C1), 68.6 (C2), 68.5 (Cp), 68.1 (C3), 48.8 (C4), 48.1 (C8), 43.1 (C5), 27.3 (C7), 26.1 (C6). IR (ATR): ν 3227 (w), 2918 (w), 2847 (w), 1581 (s), 1429 (m), 1384 (w), 1358 (m), 1330 (m), 1277 (m), 1232 (m), 1198 (w), 1139 (m), 1091 (m), 1077 (m), 1019 (w), 1000 (m), 971 (m), 871 (s), 850 (m), 801 (s), 765 (m), 642 (m) [cm^{-1}]. Anal. Calcd for $C_{24}H_{26}ClFeN_3$: C, 64.37, H, 5.85, N, 9.38. Found: C, 64.01, H, 6.11, N, 8.98. ESI-MS (HR) calculated for $C_{24}H_{27}ClFeN_3^+$: 448.1243. Found: 448.1249 $[M + H]^+$.

***N*-(7-Chloro-4-quinolyl)-*N*′-ferrocenyl-propane-1,2-diamine (4d).** This product was obtained as a yellow solid (0.366 g, 0.84 mmol, 84%). ^{1}H NMR (300 MHz, $CDCl_3$): δ (ppm) 8.53 (d, ^3J = 5.3 Hz, 1H, 10-H), 7.96 (d, ^4J = 2.0 Hz, 1H, 12-H), 7.66 (d, ^3J = 8.9 Hz, 1H, 15-H), 7.36 (dd, ^3J = 8.9 Hz, ^4J = 2.0 Hz, 1H, 14-H), 6.37 (d, ^3J = 5.5 Hz, 1H, 9-H), 5.94 (br s, 1H, Ar-N*H*-), 4.21 (s, 1H, 2-H), 4.18 (s, 1H, 3-H), 4.14 (s, 2H, 2′,3′-H), 4.13 (s, 5H, Cp-H), 3.59 (m, 2H, 4-H), 3.32 (m, 1H, 5-H), 3.15 (m, 1H, 5′-H), 3.02 (m, 1H, 6-H), 1.58 (br s, 1H, CH_2NHCH_2), 1.27 (d, ^3J = 6.1 Hz, 3H, 7-H). ^{13}C NMR (75 MHz, $CDCl_3$): δ (ppm) 150.8 (C10), 150.3 (C8), 141.9 (C11), 135.6 (C13), 126.9 (C12), 125.6 (C14), 122.2 (C15), 117.1 (C16), 98.6 (C9), 89.9 (C1), 68.8 (C2), 68.6 (Cp), 68.4 (C3), 50.5 (C4), 46.7 (C6), 45.4 (C5), 17.5 (C7). IR (ATR): ν 3286 (b), 3087 (w), 2918 (w), 2849 (w), 1576 (s), 1528 (m), 1447 (m), 1368 (m), 1330 (m), 1275 (w), 1238 (m), 1200 (w), 1134 (m), 1104 (m), 1077 (m), 999 (m), 876 (m), 847 (m), 803 (s), 765 (m), 642 (m) [cm^{-1}]. Anal. Calcd for $C_{23}H_{24}ClFeN_3$: C, 63.69, H, 5.58, N, 9.69. Found: C, 63.69, H, 5.94, N, 9.55. ESI-MS (HR) calculated for $C_{23}H_{25}ClFeN_3^+$: 434.1086. Found: 434.1090 $[M + H]^+$.

***N*-(7-Chloro-4-quinolyl)-*N*′-ferrocenyl-2,2-dimethylpropane-1,3-diamine (4e).** This product was obtained as a light yellow solid (0.313 g, 0.68 mmol, 68%). ^{1}H NMR (300 MHz, $CDCl_3$): δ (ppm) 8.56 (br, 1H, Ar-N*H*-), 8.47 (d, ^3J = 5.4 Hz, 1H, 12-H), 7.90 (d, ^4J = 2.0 Hz, 1H, 14-H), 7.60 (d, ^3J = 8.9 Hz, 1H, 17-H), 7.19 (dd, ^3J = 8.9 Hz, ^4J = 2.0 Hz, 1H, 16-H), 6.25 (d, ^3J = 5.4 Hz, 1H, 11-H), 4.24 (m, 2H, 2-H), 4.23 (m, 2H, 3-H), 4.15 (s, 5H, Cp-H), 3.58 (br, 2H, 4-H), 3.14 (m, 2H, 7-H), 2.77 (br, 2H, 5-H), 1.50 (vb, 1H, CH_2NHCH_2), 1.09 (s, 6H, 8,9-H). ^{13}C NMR (75 MHz, $CDCl_3$): δ (ppm) 152.4 (C12), 151.1 (C10), 149.4 (C13), 134.6 (C15), 128.6 (C14), 125.0 (C16), 123.0 (C17), 117.0 (C18), 97.9 (C11), 85.9 (C1), 69.1 (C2), 68.7 (Cp), 68.5 (C3), 61.3 (C7), 56.1 (C4), 50.4 (C5), 33.8 (C6), 25.2 (C8-9). IR (ATR): ν 3081 (w), 2952 (w), 1578 (s), 1465 (m), 1444 (m), 1432 (m), 1380 (w), 1361 (m), 1330 (m), 1310 (m), 1272 (w), 1232 (w), 1202 (w), 1166 (w), 1137 (m), 1086 (m), 1030 (m), 999 (w), 901 (m), 849 (m), 801 (s), 768 (m), 701 (m), 645 (m) [cm^{-1}]. Anal. Calcd for $C_{25}H_{28}ClFeN_3$: C, 65.02, H, 6.11, N, 9.10. Found: C, 64.91, H, 6.38, N, 8.62. ESI-MS (HR) calculated for $C_{25}H_{29}ClFeN_3^+$: 462.1399. Found: 462.1413 $[M + H]^+$.

General Procedure for the Synthesis of Bridged Ferrocenyl 4-Aminoquinoline Derivatives (5a–e). *Method A.* 1,1′-Bis(*N*,*N*′-trimethylaminomethyl)ferrocene iodide **2** (0.10 g, 0.17 mmol, 1 equiv), the corresponding 4-aminoquinoline derivatives **3a–e** (0.34 mmol, 2 equiv), and NaOH (0.04 g, 1 mmol, 6 equiv) were combined with 20 mL of acetonitrile in a 20 mL microwave vial. The reaction was carried out in a microwave reactor for 6 h at 110 °C. The solvent was removed under reduced pressure.

dx.doi.org/10.1021/jm301422h | J. Med. Chem. XXXX, XXX, XXX–XXX

Method B. 1,1′-Bis(*N*,*N*′-trimethylaminomethyl)ferrocene iodide **2** (0.10 g, 0.17 mmol, 1 equiv), the corresponding 4-aminoquinoline derivatives **3a−e** (0.34 mmol, 2 equiv), and NaOH (0.04 g, 1 mmol, 6 equiv) were refluxed in acetonitrile (20 mL) for 48 h. Semipurification of the desired product was done by flash column chromatography on silica (**5a,b,d,e**) or on preparative TLC silica gel plate (**5c**) with an acetone/dichloromethane/triethylamine (5:4:1) mixture as eluent. The products were purified to >95% by HPLC using a linear gradient of 100% water to 100% acetonitrile.

***N*-{[*N*′-(7-Chloroquinolin-4-yl)]ethane-1,2-diamine}-1,1′-(*N*,*N*-dimethane-yl)ferrocene (5a).** This product was obtained as a yellow solid (0.016 g, 0.037 mmol, 22%). ^{1}H NMR (600 MHz, CD_3OD): δ (ppm) 8.41 (d, ^3J = 5.6 Hz, 1H, 9-H), 8.13 (d, 3J = 8.7 Hz, 1H, 14-H), 7.82 (d, ^4J = 2.0 Hz, 1H, 11-H), 7.49 (dd, ^3J = 8.7, ^4J = 2.0 Hz, 1H, 13-H), 6.66 (d, ^3J = 5.6 Hz, 1H, 8-H), 4.10 (t, 4H, 2-H), 4.07 (t, 4H, 3-H), 3.65 (t, ^3J = 6.4 Hz, 2H, 6-H), 3.13 (t, ^3J = 6.7 Hz, 2H, 5-H), 3.06 (br s, 4H, 4-H). ^{13}C NMR (151 MHz, CD_3OD): δ (ppm) 158.4 (C7), 149.4 (C9), 148.8 (C15), 133.4 (C10), 124.0 (C11), 123.0 (C13), 120.6 (C14), 115. 4 (C12), 96.6 (C8), 80.7 (C1), 67.5 (C3), 66.8 (C2), 52.8 (C5), 49.7 (C4), 38.5 (C6). IR (ATR): ν 3228 (w), 3014 (w), 2958 (w), 2918 (m), 2180 (w), 1659 (m), 1613 (m), 1580 (s), 1453 (m), 1433 (m), 1380 (m), 1302 (m), 1228 (m), 1149 (m), 1112 (m), 1086 (w), 1026 (m), 969 (w), 930 (w), 901 (w), 877 (m), 849 (m), 797 (s), 646 (m) [cm^{-1}]. ESI-MS (HR) calculated for $C_{23}H_{23}ClFeN_3^+$: 432.0930. Found: 432.0927 $[M + H]^+$.

***N*-{[*N*′-(7-Chloroquinolin-4-yl)]propane-1,3-diamine}-1,1′-(*N*,*N*-dimethane-yl)ferrocene (5b).** This compound can be further purified by recrystallization in an acetone/dichloromethane (1:1) mixture, yielding orange crystals (0.015 g, 0.03 mmol, 20%). ^{1}H NMR (600 MHz, CD_3OD): δ (ppm) 8.37 (d, ^3J = 5.6 Hz, 1H, 10-H), 8.14 (d, ^3J = 8.7 Hz, 1H, 15-H), 7.78 (d, ^4J = 2.0 Hz, 1H, 12-H), 7.42 (dd, ^3J = 8.7 Hz, ^4J = 2.0 Hz, 1H, 14-H), 6.63 (d, ^3J = 5.6 Hz, 1H, 9-H), 4.10 (t, 4H, 2-H), 4.05 (t, 4H, 3-H), 3.54 (t, 2H, 5-H), 2.96 (br s, 4H, 4-H), 2.87 (t, 2H, 7-H), 2.09 (m, 2H, 6-H). ^{13}C NMR (151 MHz, CD_3OD): δ (ppm) 153.4 (C8), 152.4 (C10), 149.7 (C16), 136.8 (C11), 127.6 (C12), 126.4 (C14), 124.7 (C15), 119.0 (C13), 100.0 (C9), 84.3 (C1), 71.2 (C2), 70.5 (C3), 56.5 (C7), 53.5 (C4), 42.6 (C5), 27.7 (C6). IR (ATR): ν 3226 (w), 3092 (w), 2919 (s), 2850 (m), 2188 (w), 1611 (m), 1575 (s), 1452 (s), 1367 (m), 1318 (w), 1282 (w), 1238 (w), 1214 (m), 1168 (m), 1103 (m), 1027 (m), 964 (w), 930 (w), 902 (w), 880 (m), 849 (m), 801 (s), 768 (m) [cm^{-1}]. ESI-MS (HR) calculated for $C_{24}H_{25}ClFeN_3^+$: 446.1086. Found: 446.1093 $[M + H]^+$.

***N*-{[*N*′-(7-Chloroquinolin-4-yl)]butane-1,4-diamine}-1,1′-(*N*,*N*-dimethane-yl)ferrocene (5c).** This product was obtained as a yellow solid (0.015 g, 0.033 mmol, 19%). ^{1}H NMR (400 MHz, CD_3OD): δ (ppm) 8.38 (d, ^3J = 6.0 Hz, 1H, 11-H), 8.19 (d, ^3J = 8.8 Hz, 1H, 16-H), 7.80 (d, ^4J = 2.2 Hz, 1H, 13-H), 7.48 (dd, ^3J = 9.1, ^4J = 2.2 Hz, 1H, 15-H), 6.67 (d, ^3J = 6.2 Hz, 1H, 10-H), 4.10 (m, 4H, 2-H), 4.07 (m, 4H, 3-H), 3.53 (m, 2H, 8-H), 3.04 (br s, 4H, 4-H), 2.89 (m, 2H, 5-H), 1.94 (s, 2H, 7-H), 1.88 (m, 2H, 6-H). ^{13}C NMR (101 MHz, CD_3OD): δ (ppm) 152.6 (C9), 149.2 (C11), 146.5 (C17), 136.1 (C14), 125.4 (C15), 124.8 (C13), 123.4 (C16), 117.5 (C12), 98.5 (C10), 81.8 (C1), 69.7 (C2), 69.2 (C3), 57.1 (C5), 51.7 (C4), 42.8 (C8), 26.0 (C7), 24.3 (C6). IR (ATR): ν 3234 (w), 3190 (w), 2919 (m), 2850 (m), 2182 (w), 1664 (m), 1610 (m), 1578 (s), 1450 (m), 1430 (m), 1367 (m), 1334 (m), 1279 (w), 1254 (w), 1212 (w), 1200 (w), 1100 (m), 1078 (m), 1027 (m), 848 (m), 803 (s), 765 (m) [cm^{-1}]. ESI-MS (HR) calculated for $C_{25}H_{27}ClFeN_3^+$: 460.1243. Found: 460.1255 $[M + H]^+$.

***N*-{[*N*′-(7-Chloroquinolin-4-yl)]propane-1,2-diamine}-1,1′-(*N*,*N*-dimethane-yl)ferrocene (5d).** This product was obtained as a yellow solid (0.018 g, 0.04 mmol, 23%). ^{1}H NMR (600 MHz, CD_3OD): δ (ppm) 8.41 (d, ^3J = 5.4 Hz, 1H, 10-H), 8.13 (d, ^3J = 8.9 Hz, 1H, 15-H), 7.84 (d, ^4J = 2.3 Hz, 1H, 12-H), 7.53 (dd, ^3J = 8.9, ^4J = 1.9 Hz, 1H, 14-H), 6.61 (d, ^3J = 5.4 Hz, 1H, 9-H), 4.17 (m, 2H, 2-H), 4.07 (m, 2H, 2′-H), 4.02 (m, 2H, 3-H), 3.99 (m, 2H, 3′-H), 3.57 (m, 1H, 6-H), 3.46 (m, 2H, 5-H), 3.20 (m, 2H, 4-H), 2.99 (m, 2H, 4′-H), 1.26 (d, ^2J = 6.6 Hz, 3H, 7-H). ^{13}C NMR (151 MHz, CD_3OD): δ (ppm) 157.9 (C8), 152.8 (C10), 150.0 (C16), 136.9 (C11), 128.1 (C12), 126.6 (C14), 123.9 (C15), 118.8 (C13), 100.5 (C9), 84.5 (C1), 71.2 (C2), 71.0 (C2′), 70.4 (C3, C3′), 59.7 (C4), 47.5 (C5), 31.2 (C6), 12.5 (C7). IR (ATR): ν 3380 (w), 2918 (m), 2849 (m), 2181 (w), 1664 (m), 1608 (m), 1579 (s), 1524 (m), 1470 (m), 1448 (m), 1379 (m), 1331 (m), 1298 (w), 1260 (w), 1234 (m), 1158 (m), 1088 (m), 1028 (m), 966 (w), 940 (w), 924 (w), 878 (m), 848 (m), 801 (s), 760 (m) [cm^{-1}]. ESI-MS (HR) calculated for $C_{24}H_{25}ClFeN_3^+$: 446.1086. Found: 446.1075 $[M + H]^+$.

***N*-{[*N*′-(7-Chloroquinolin-4-yl)]-2,2-dimethylpropane-1,3-diamine}-1,1′-(*N*,*N*-dimethane-yl)ferrocene (5e).** This product was obtained as a yellow solid (0.004 g, 0.009 mmol, 5%). ^{1}H NMR (400 MHz, CD_3OD): δ (ppm) 8.39 (d, ^3J = 6.1 Hz, 1H, 12-H), 8.25 (d, ^3J = 8.9 Hz, 1H, 17-H), 7.82 (d, ^4J = 2.4 Hz, 1H, 14-H), 7.50 (dd, ^3J = 8.9, ^4J = 2.0 Hz, 1H, 16-H), 6.76 (d, ^3J = 6.1 Hz, 1H, 11-H), 4.13 (m, 4H, 2-H), 4.08 (m, 4H, 3-H), 3.46 (m, 2H, 5-H), 3.04 (m, 2H, 7-H), 2.69 (m,4H, 4-H), 1.16 (s, 6H, 8,9-H). ^{13}C NMR (101 MHz, CD_3OD): δ (ppm) 161.8 (C10), 156.3 (C12), 148.4 (C18), 136.8 (C13), 129.0 (C14), 126.6 (C16), 124.6 (C17), 122.1 (C15), 100.3 (C9), 85.6 (C1), 70.7 (C2), 70.2 (C3), 61.7 (C4), 52.7 (C7), 39.9 (C5), 32.2 (C6), 14.6 (C8,9). IR (ATR): ν 3346 (w), 3180 (w), 2878 (m), 2182 (w), 1670 (m), 1600 (m), 1576 (s), 1520 (m), 1460 (m), 1438 (m), 1374 (m), 1330 (m), 1294 (w), 1260 (w), 1222 (m), 1146 (m), 1088 (m), 1020 (m), 956 (m), 936 (w), 838 (m), 804 (s), 765 (m) [cm^{-1}]. ESI-MS (HR) calculated for $C_{26}H_{29}ClFeN_3^+$: 474.1399. Found: 474.1398 $[M + H]^+$.

In Vitro Antiplasmodial Activity Studies. The test samples were tested in triplicate on one, two, or three occasions against the chloroquine-sensitive (CQS) D10 strain and the chloroquine-resistant (CQR) Dd2 and K1 strains of *Plasmodium falciparum*. Continuous in vitro cultures of asexual erythrocyte stages of *P. falciparum* were maintained using a modified method of Trager and Jensen.[69] Quantitative assessment of antiplasmodial activity in vitro was determined via the parasite lactate dehydrogenase assay using a modified method described by Makler.[70] The test samples were prepared as a 2 mg/mL stock solution in 10% DMSO or 20 mg/mL in 100% DMSO and sonicated to enhance solubility. Samples of **4b**, **4d**, **4e**, and **5b** were used as suspensions in the assay, leading to a tendency to underestimate the IC_{50} values, so the given results are conservative calculations. Stock solutions were stored at −20 °C. Further dilutions were prepared on the day of the experiment. Chloroquine (CQ) was used as the reference drug in all experiments. Test samples were initially tested at three concentrations (10, 5, and 2.5 μg/mL). CQ was tested at three concentrations (30, 15, and 7.5 ng/mL). A full dose−response was performed for all compounds to determine the concentration inhibiting 50% of parasite growth (IC_{50}). For D10, test samples were tested at a starting concentration of 100 μg/mL, which was then serially diluted 2-fold in complete medium to give 10 concentrations, with the lowest concentration being 0.2 μg/mL. The same dilution technique was used for all samples. CQ was tested at a starting concentration of 100 ng/mL. Several compounds were retested at a starting concentration of either 1000 ng/mL or 100 ng/mL. For Dd2 and K1, samples were tested at a starting concentration of 1000 ng/mL, which was then serially diluted 2-fold in complete medium to give 10 concentrations, with the lowest concentration being 2 ng/mL. The same dilution technique was used for all samples. CQ was tested at a starting concentration of 1000 ng/mL. The highest concentration of solvent to which the parasites were exposed had no measurable effect on the parasite viability (data not shown). The IC_{50} values were obtained using a nonlinear dose−response curve fitting analysis via Graph Pad Prism, version 4.0, software.

In Vitro Antitumor Activity and Cytotoxicity Assay. Human breast cancer cells MDA-MB-435S (HTB-129) were purchased from ATCC. Cells were grown as monolayers in medium (89% Leibovitz's L-15 medium with 2 mM L-glutamine, 0.01 mg/mL bovine insulin, 1% penicillin/streptomycin, and 10% fetal bovine serum) and maintained at 37 °C in a humidified atmosphere. Human normal breast epithelial cells MCF-10A (CRL-10317) were purchased from ATCC. Cells were grown as monolayers in medium (93% Dulbecco's modified Eagle medium F12, 5% fetal bovine serum, 1% penicillin/streptomycin, 1% 2 mM glutamine, 0.01 μg/mL human epidermal growth factor, 0.5 μg/mL

dx.doi.org/10.1021/jm301422h | J. Med. Chem. XXXX, XXX, XXX−XXX

hydrocortisone, 10 μg/mL insulin) and maintained at 37 °C in a humidified atmosphere containing 5% CO_2. Cell growth inhibition was assessed using the colorimetric cell proliferation MTT assay.[43] Cells were detached from culture flasks with 0.25% trypsin and 0.03% EDTA (Sigma) and resuspended in fresh culture medium at a density of 3×10^5 cells/mL (MDA-MB435S) or 1×10^5 cells/mL (MCF-10A). By use of a Falcon 96-well, flat-bottom plate, 100 μL of the cell suspension was added to each of the wells. The cells were incubated for 24 h, after which time the cells were treated with each compound (in triplicate) at concentrations ranging from 0.1 to 200 μg/mL. To assist dissolution, the complexes were first dissolved in DMSO to provide stock solutions and then serially diluted with medium to give the final concentrations (final concentration of DMSO was 0.5%). A stock solution of chloroquine diphosphate salt was prepared in 0.5% DMSO in medium and serially diluted. Cisplatin was used as positive control, and stock solutions were prepared in 0.5% DMSO in medium and serially diluted. After incubation with the compounds for 72 h, 50 μL of a 2.5 mg/mL solution of MTT in PBS was added to each well and further incubated for 3−4 h. The supernatant was removed, and the cells were dissolved in 150 μL of DMSO. Cell survival was determined by means of metabolic reduction of MTT. Optical density from the MTT assay was measured at 570 nm on a Beckman Coulter DTX 880 multimode detector. Absorbance values were corrected to the control and blank. Tests were run in duplicate or triplicate. The IC_{50} values were obtained from plots of cell survival (%) against log of drug concentration using a nonlinear dose−response curve fitting analysis via Graph Pad Prism, version 4.0, software.

Hematin Association Assay. The association constants of the studied compounds with hematin were measured as described previously in the literature.[50] Hemin (bovine, ≥90.0%) was obtained from Sigma-Aldrich, and a stock solution was prepared by dissolving 6−8 mg of hemin in 10 mL of AR grade DMSO and stored in the dark. The working hemin solution (2 μM) was prepared fresh from 20 μL of the hemin stock solution diluted to a final volume of 10 mL with the buffered solution (40% v/v DMSO, 0.020 M HEPES, apparent pH 7.5). Hematin−compound interactions were monitored by titrating the hematin solution with each compound and measuring the absorbance of the Soret band at 402 nm. In a UV−vis cell, 2 mL of the 2 μM hematin solution was titrated with a 2 mM solution of the compound in the same buffered solution (40% v/v DMSO, 0.020 M HEPES, apparent pH 7.5). The temperature was maintained at 25 °C using a water circulating bath in a thermostated cell holder, and absorbance readings were recorded for each addition, after 5 min of stabilization, using a Hewlett-Packard 8543 diode array spectrophotometer outfitted with a Fisher Scientific 1016D Isotemp thermostated water cooling system. Absorbance data were collected using the Agilent 845x UV−visible spectroscopy system (Agilent Technologies, Inc., 2003−2008). Different concentrations of compound were analyzed (0, 1, 3, 5, 10, 15, 20, 25, 30, 35, 40, 50, 60, 70, 80, 90, and 100 equiv of hematin). A reference cell with the buffered solution (40% v/v DMSO, 0.020 M HEPES, apparent pH 7.5) was also titrated with the same equivalent of each compound in order to zero the absorbance of the drug. Titrations were repeated in triplicate for each compound and blank. Absorbance data were corrected for dilution, analyzed at 402 nm, and fitted to a 1:1 association model using nonlinear least-squares fitting analysis via Graph Pad Prism, version 4.0, software to obtain the association constant (reported as log K). Graphs were produced using the OriginPro 7.5 software.

***β*-Hematin Formation Inhibition Assay.** The inhibition of *β*-hematin formation was assayed as described previously in the literature.[51] A 12.9 M acetate stock solution was prepared using sodium acetate trihydrate[51] and kept at 70 °C throughout the experiment. The pH of the stock solution was measured as 5.05. A 1.68 mM stock solution of hematin was prepared by dissolving 5.5 mg of hemin (bovine, ≥90.0%, obtained from Sigma-Aldrich) in 5.0 mL of 0.1 M NaOH. Stock solutions of each compound were prepared in DMSO in concentrations that ranged from 0.15 to 0.20 M. Hematin stock solution (20.2 μL, 0.035 μmol) was dispensed to a series of Eppendorf tubes (11 tubes for each compound tested). The 0.1 M NaOH solution was neutralized with 2.02 μL of 1.0 M HCl prior to the addition of the compounds. Predetermined volumes of the stock solution of the test compounds were added to give 0−10 equiv relative to hematin in the final solution. After mixing, 11.74 μL of the 12.9 M acetate solution maintained at 70 °C was added to each Eppendorf tube. The final hematin concentration was 1 mM, and the final solution pH was 4.5. The vortexed solutions were then incubated at 60 °C for 1 h. The solutions were quenched at room temperature with 900 μL of a 5% pyridine solution (200 mM HEPES, pH 8.2), followed by addition of 1100 μL of 5% pyridine solution (20 mM HEPES, pH 7.5). Each tube was vortexed to ensure the complete dissolution of hematin and then allowed to settle for 30 min at room temperature. The supernatant was transferred to a cuvette without disturbing the precipitate. Absorbances were read at 405 nm at a Cary 100 Bio (Varian) UV−visible spectrophotometer. Graphs were produced using the OriginPro 7.5 software.

Partition Coefficient and Molecular Shape Analysis. Theoretical log *P* values were calculated using the commercially available ACD/Labs 11.0 program. Molecular modeling was performed using the Gaussian 09 and GaussView packages (Gaussian, Inc.). Density functional theory (DFT), with the B3LYP functional employing the 6-31+G(d,p) basis set, was used to obtain the optimized geometry and the electron density. Frequency calculations were performed to verify that the optimized structures were a minima, having no imaginary frequencies. The electrostatic potential was mapped onto the calculated electron density surface. Molden package software was used to obtain the topological polar surface area (tPSA) from the optimized structures.

■ ASSOCIATED CONTENT

Ⓢ Supporting Information

Additional ^{1}H NMR data, ^{1}H NMR spectra, antiplasmodial data, survival and association plots, therapeutic indices, and molecular electronic potential surfaces. This material is available free of charge via the Internet at http://pubs.acs.org.

■ AUTHOR INFORMATION

Corresponding Author

*Phone: 604-822-4449. E-mail: orvig@chem.ubc.ca.

Notes

The authors declare no competing financial interest.

■ ACKNOWLEDGMENTS

The authors thank Dr. Elena Polishchuk from UBC Biological Services for her advice and support. We are grateful for a Discovery grant from the Natural Sciences and Engineering Research Council of Canada (NSERC) and support from Advanced Applied Physics Solutions (AAPS) C.O. acknowledges the Canada Council for the Arts for a Killam Research Fellowship (2011−2013).

■ ABBREVIATIONS USED

Cp, cyclopentadienyl; CQ, chloroquine; CQR, chloroquine-resistant; CQS, chloroquine-sensitive; DMSO, dimethylsulfoxide; Fe(III)PPIX, ferriprotoporphyrin IX; FQ, ferroquine; HEPES, 2-[4-(2-hydroxyethyl)piperazin-1-yl]ethanesulfonic acid; IC_{50}, half-maximum inhibitory concentration; ClogP, calculated partition coefficient; MeI, iodomethane; MeOH, methanol; MEP, molecular electrostatic potential; MFA, molecular field analysis; MSA, molecular shape analysis; *n*-BuLi, *n*-butyllithium; NMR, nuclear magnetic resonance; tPSA, topological polar surface area; 3D-QSAR, three dimensional quantitative structure−activity relationship; RI, resistance index; rt, room temperature; SAR, structure−activity relationship; TEA, triethylamine; TFA, trifluoroacetic acid; THF, tetrahydrofuran; TI, therapeutic index; TLC, thin layer chromatography; TMEDA, *N*,*N*,*N*′,*N*′-tetramethylethylenediamine; WHO, World Health Organization

REFERENCES

(1) World Health Organization. *World Malaria Report 2011*; WHO Press: Geneva, 2012.

(2) Murray, C. J. L.; Rosenfeld, L. C.; Lim, S. S.; Andrews, K. G.; Foreman, K. J.; Haring, D.; Fullman, N.; Naghavi, M.; Lozano, R.; Lopez, A. D. Global malaria mortality between 1980 and 2010: a systematic analysis. *Lancet* **2012**, *379*, 413−431.

(3) World Health Organization. *Global Plan for Artemisinin Resistance Containment (GPARC)*; WHO Press: Geneva, 2011.

(4) Biot, C.; Glorian, G.; Maciejewski, L. A.; Brocard, J. S.; Domarle, O.; Blampain, G.; Millet, P.; Georges, A. J.; Abessolo, H.; Dive, D.; Lebibi, J. Synthesis and antimalarial activity in vitro and in vivo of a new ferrocene-chloroquine analogue. *J. Med. Chem.* **1997**, *40*, 3715−3718.

(5) Domarle, O.; Blampain, G.; Agnaniet, H.; Nzadiyabi, T.; Lebibi, J.; Brocard, J.; Maciejewski, L.; Biot, C.; Georges, A. J.; Millet, P. In vitro antimalarial activity of a new organometallic analog, ferrocene-chloroquine. *Antimicrob. Agents Chemother.* **1998**, *42*, 540−544.

(6) Biot, C.; Delhaes, L.; Abessolo, H.; Domarle, O.; Maciejewski, L. A.; Mortuaire, M.; Delcourt, P.; Deloron, P.; Camus, D.; Dive, D.; Brocard, J. S. Novel metallocenic compounds as antimalarial agents. Study of the position of ferrocene in chloroquine. *J. Organomet. Chem.* **1999**, *589*, 59−65.

(7) Biot, C.; Daher, W.; Ndiaye, C. M.; Melnyk, P.; Pradines, B.; Chavain, N.; Pellet, A.; Fraisse, L.; Pelinski, L.; Jarry, C.; Brocard, J.; Khalife, J.; Forfar-Bares, I.; Dive, D. Probing the role of the covalent linkage of ferrocene into a chloroquine template. *J. Med. Chem.* **2006**, *49*, 4707−4714.

(8) Beagley, P.; Blackie, M. A. L.; Chibale, K.; Clarkson, C.; Moss, J. R.; Smith, P. J. Synthesis and antimalarial activity in vitro of new ruthenocene−chloroquine analogues. *J. Chem. Soc., Dalton Trans.* **2002**, 4426−4433.

(9) Mombo-Ngoma, G.; Supan, C.; Dal-Bianco, M. P.; Missinou, M. A.; Matsiegui, P.-B.; Salazar, C. L. O.; Issifou, S.; Ter-Minassian, D.; Ramharter, M.; Kombila, M.; Kremsner, P. G.; Lell, B. Phase I randomized dose-ascending placebo-controlled trials of ferroquine—a candidate anti-malarial drug—in adults with asymptomatic *Plasmodium falciparum* infection. *Malar. J.* **2011**, *10*, 53.

(10) Blackie, M. A. L.; Beagley, P.; Croft, S. L.; Kendrick, H.; Moss, J. R.; Chibale, K. Metallocene-based antimalarials: an exploration into the influence of the ferrocenyl moiety on in vitro antimalarial activity in chloroquine-sensitive and chloroquine-resistant strains of *Plasmodium falciparum*. *Bioorg. Med. Chem.* **2007**, *15*, 6510−6516.

(11) Beagley, P.; Blackie, M. A. L.; Chibale, K.; Clarkson, C.; Meijboom, R.; Moss, J. R.; Smith, P. J.; Su, H. Synthesis and antiplasmodial activity in vitro of new ferrocene−chloroquine analogues. *Dalton Trans.* **2003**, 3046−3051.

(12) Biot, C.; Daher, W.; Chavain, N.; Fandeur, T.; Khalife, J.; Dive, D.; De Clercq, E. Design and synthesis of hydroxyferroquine derivatives with antimalarial and antiviral activities. *J. Med. Chem.* **2006**, *49*, 2845−2849.

(13) Chibale, K.; Moss, J. R.; Blackie, M.; van Schalkwyk, D.; Smith, P. J. New amine and urea analogs of ferrochloroquine: synthesis, antimalarial activity in vitro and electrochemical studies. *Tetrahedron Lett.* **2000**, *41*, 6231−6235.

(14) Dive, D.; Biot, C. Ferrocene conjugates of chloroquine and other antimalarials: the development of ferroquine, a new antimalarial. *ChemMedChem* **2008**, *3*, 383−391.

(15) Biot, C. Ferroquine: a new weapon in the fight against malaria. *Curr. Med. Chem.: Anti-Infect. Agents* **2004**, *3*, 135−147.

(16) Blackie, M. A. L.; Chibale, K. Metallocene antimalarials: the continuing quest. *Met.-Based Drugs* **2008**, *2008*, 495123.

(17) Biot, C.; Taramelli, D.; Forfar-Bares, I.; Maciejewski, L. A.; Boyce, M.; Nowogrocki, G.; Brocard, J. S.; Basilico, N.; Olliaro, P.; Egan, T. J. Insights into the mechanism of action of ferroquine. Relationship between physicochemical properties and antiplasmodial activity. *Mol. Pharmaceutics* **2005**, *2*, 185−193.

(18) Biot, C.; Dive, D. Bioorganometallic Chemistry and Malaria. In *Medicinal Organometallic Chemistry*; Jaouen, G., Metzler-Nolte, N., Eds.; Topics in Organometallic Chemistry, Vol. *32*; Springer: Berlin, 2010; pp 155−193.

(19) Olliaro, P. Mode of action and mechanisms of resistance for antimalarial drugs. *Pharmacol. Ther.* **2001**, *89*, 207−219.

(20) Dubar, F.; Khalife, J.; Brocard, J.; Dive, D.; Biot, C. Ferroquine, an ingenious antimalarial drug—thoughts on the mechanism of action. *Molecules* **2008**, *13*, 2900−2907.

(21) Dubar, F.; Egan, T. J.; Pradines, B.; Kuter, D.; Ncokazi, K. K.; Forge, D.; Paul, J.-F.; Pierrot, C.; Kalamou, H.; Khalife, J.; Buisine, E.; Rogier, C.; Vezin, H.; Forfar, I.; Slomianny, C.; Trivelli, X.; Kapishnikov, S.; Leiserowitz, L.; Dive, D.; Biot, C. The antimalarial ferroquine: role of the metal and intramolecular hydrogen bond in activity and resistance. *ACS Chem. Biol.* **2011**, *6*, 275−287.

(22) Chavain, N.; Vezin, H.; Dive, D.; Touati, N.; Paul, J.-F.; Buisine, E.; Biot, C. Investigation of the redox behavior of ferroquine, a new antimalarial. *Mol. Pharmaceutics* **2008**, *5*, 710−716.

(23) Biot, C.; Dubar, F.; Khalife, J.; Slomianny, C. Opening up the advantages of the ruthenocenic bioprobes of ferroquine: distribution and localization in *Plasmodium falciparum*-infected erythrocytes. *Metallomics* **2012**, *4*, 780−783.

(24) Ridley, R. G.; Hofheinz, W.; Matile, H.; Jaquet, C.; Dorn, A.; Masciadri, R.; Jolidon, S.; Richter, W. F.; Guenzi, A.; Girometta, M. A.; Urwyler, H.; Huber, W.; Thaitong, S.; Peters, W. 4-Aminoquinoline Analogs of Chloroquine with Shortened Side Chains Retain Activity against Chloroquine-Resistant *Plasmodium falciparum*. *Antimicrob. Agents Chemother.* **1996**, *40*, 1846−1854.

(25) De, D.; Krogstad, F. M.; Cogswell, F. B.; Krogstad, D. J. Aminoquinolines that circumvent resistance in *Plasmodium falciparum* in vitro. *Am. J. Trop. Med.* **1996**, *55*, 579−583.

(26) Stocks, P. A.; Raynes, K. J.; Bray, P. G.; Park, B. K.; O'Neill, P. M.; Ward, S. A. Novel short chain chloroquine analogues retain activity against chloroquine resistant K1 *Plasmodium falciparum*. *J. Med. Chem.* **2002**, *45*, 4975−4983.

(27) De, D.; Krogstad, F. M.; Byers, L. D.; Krogstad, D. J. Structure−activity relationships for antiplasmodial activity among 7-substituted 4-aminoquinolines. *J. Med. Chem.* **1998**, *41*, 4918−4926.

(28) Egan, T. J.; Hunter, R.; Kaschula, C. H.; Marques, H. M.; Misplon, A.; Walden, J. Structure−function relationships in aminoquinolines: effect of amino and chloro groups on quinoline-hematin complex formation, inhibition of β-hematin formation, and antiplasmodial activity. *J. Med. Chem.* **2000**, *43*, 283−291.

(29) Madrid, P. B.; Wilson, N. T.; DeRisi, J. L.; Guy, R. K. Parallel synthesis and antimalarial screening of a 4-aminoquinoline library. *J. Comb. Chem.* **2004**, *6*, 437−442.

(30) Solomon, V. R.; Puri, S. K.; Srivastava, K.; Katti, S. B. Design and synthesis of new antimalarial agents from 4-aminoquinoline. *Bioorg. Med. Chem.* **2005**, *13*, 2157−2165.

(31) Madrid, P. B.; Liou, A. P.; DeRisi, J. L.; Guy, R. K. Incorporation of an intramolecular hydrogen-bonding motif in the side chain of 4-aminoquinolines enhances activity against drug-resistant *P. falciparum*. *J. Med. Chem.* **2006**, *49*, 4535−4543.

(32) Musonda, C. C.; Taylor, D.; Lehman, J.; Gut, J.; Rosenthal, P. J.; Chibale, K. Application of multi-component reactions to antimalarial drug discovery. Part 1: Parallel synthesis and antiplasmodial activity of new 4-aminoquinoline Ugi adducts. *Bioorg. Med. Chem. Lett.* **2004**, *14*, 3901−3905.

(33) Osgerby, J. M. Ferrocene derivatives. Part VI. DL-Ferrocenylalanine. *J. Chem. Soc.* **1958**, 656−660.

(34) Grossel, M. C.; Hamilton, D. G.; Fuller, J. I.; Millan-Barios, E. Alkali-metal binding properties of simple ferrocenyl- and ruthenocenyl-substituted aza-crown ethers. *J. Chem. Soc., Dalton Trans.* **1997**, *19*, 3471−3477.

(35) Bildstein, B.; Malaun, M.; Kopacka, H.; Ongania, K.; Wurst, K. Imidazoline-2-ylidene metal complexes with pendant ferrocenyl substituents. *J. Organomet. Chem.* **1998**, *552*, 45−61.

(36) Herrmann, C.; Salas, P. F.; Patrick, B. O.; de Kock, C.; Smith, P. J.; Adam, M. J.; Orvig, C. 1,2-Disubstituted ferrocenyl carbohydrate chloroquine conjugates as potential antimalarial agents. *Dalton Trans.* **2012**, *41*, 6431−6442.

(37) N'Diaye, C. M.; Maciejewski, L. A.; Brocard, J. S.; Biot, C. Unexpected synthesis of novel aza-[3]-ferrocenophanes. *Tetrahedron Lett.* **2001**, *42*, 7221−7223.
(38) Emsley, J. Very strong hydrogen bonding. *Chem. Soc. Rev.* **1980**, *9*, 91−124.
(39) Herbert, D. E.; Ulrich, F.; Mayer, J.; Manners, I. Strained metallocenophanes and related organometallic rings containing *p*-hydrocarbon ligands and transition-metal centers. *Angew. Chem., Int. Ed.* **2007**, *46*, 5060−5081.
(40) Horie, M.; Sakano, T.; Osakada, K.; Nakao, H. A new azaferrocenophane with an azobenzene-containing ligand. Remote control of photoisomerization of the azobenzene group by redox of the iron center. *Organometallics* **2004**, *23*, 18−20.
(41) Biot, C.; Nosten, F.; Fraisse, L.; Ter-Minassian, D.; Khalife, J.; Dive, D. The antimalarial ferroquine: from bench to clinic. *Parasite* **2011**, *18*, 207−214.
(42) Martirosyan, A. R.; Rahim-Bata, R.; Freeman, A. B.; Clarke, C. D.; Howard, R. L.; Strobl, J. S. Differentiation-inducing quinolines as experimental breast cancer agents in the MCF-7 human breast cancer cell model. *Biochem. Pharmacol.* **2004**, *68*, 1729−1738.
(43) Mosmann, T. Rapid colorimetric assay for cellular growth and survival: application to proliferation and cytotoxicity assays. *J. Immunol. Methods* **1983**, *65*, 55−63.
(44) Herrmann, C.; Salas, P. F.; Cawthray, J. F.; de Kock, C.; Patrick, B. O.; Smith, P. J.; Adam, M. J.; Orvig, C. 1,1′-Disubstituted ferrocenyl carbohydrate chloroquine conjugates as potential antimalarials. *Organometallics* **2012**, *31*, 5736−5747.
(45) Herrmann, C.; Salas, P. F.; Patrick, B. O.; de Kock, C.; Smith, P. J.; Adam, M. J.; Orvig, C. Modular synthesis of 1,2- and 1,1′-disubstituted ferrocenyl carbohydrate chloroquine and mefloquine conjugates as potential antimalarial agents. *Organometallics* **2012**, *31*, 5748−5759.
(46) Egan, T. J. Interactions of quinoline antimalarials with hematin in solution. *J. Inorg. Biochem.* **2006**, *100*, 916−926.
(47) Moreau, S.; Perly, B.; Chachaty, C.; Deleuze, C. A nuclear magnetic resonance study of the interactions of antimalarial drugs with porphyrins. *Biochim. Biophys. Acta* **1985**, *840*, 107−116.
(48) Satterlee, J. D.; Constantinidis, I. UV−visible and carbon NMR studies of chloroquine binding to urohemin I chloride and uroporphyrin I in aqueous solutions. *J. Am. Chem. Soc.* **1988**, *110*, 4391−4395.
(49) Egan, T. J. Quinoline antimalarials. *Expert Opin. Ther. Pat.* **2001**, *11*, 185−209.
(50) Egan, T. J.; Mavuso, W. W.; Ross, D. C.; Marques, H. M. Thermodynamic factors controlling the interaction of quinoline antimalarial drugs with ferriprotoporphyrin IX. *J. Inorg. Biochem.* **1997**, *68*, 137−145.
(51) Ncokazi, K. K.; Egan, T. J. A colorimetric high-throughput *β*-hematin inhibition screening assay for use in the search for antimalarial compounds. *Anal. Biochem.* **2005**, *338*, 306−319.
(52) Brown, S. B.; Dean, T. C.; Jones, P. Aggregation of ferrihaems. Dimerization and protolytic equilibria of protoferrihaem and deuteroferrihaem in aqueous solution. *Biochem. J.* **1970**, *117*, 733−739.
(53) Egan, T. J.; Ncokazi, K. K. Effects of solvent composition and ionic strength on the interaction of quinoline antimalarials with ferriprotoporphyrin IX. *J. Inorg. Biochem.* **2004**, *98*, 144−152.
(54) Tilley, L.; Loria, P.; Foley, M. Chloroquine and Other Quinoline Antimalarials. In *Antimalarial Chemotherapy: Mechanisms of Action, Resistance, and New Directions in Drug Discovery*; Rosenthal, P. J., Ed.; Humana Press: Totowa, NJ, 2001; pp 87−121.
(55) Rangarajan, P. N.; Padmanaban, G. Emerging targets for antimalarial drugs. *Expert. Opin. Ther. Targets* **2001**, *5*, 423−441.
(56) ACD/Labs. http://www.acdlabs.com/home/ (accessed June 8, 2012).
(57) Ghose, A. K.; Viswanadhan, V. N.; Wendoloski, J. J. Prediction of hydrophobic (lipophilic) properties of small organic molecules using fragmental methods: an analysis of ALOGP and CLOGP methods. *J. Phys. Chem. A* **1998**, *102*, 3762−3772.
(58) Chavain, N.; Biot, C. Organometallic complexes: new tools for chemotherapy. *Curr. Med. Chem.* **2010**, *17*, 2729−2745.
(59) *MSI Cerius2*, version 4.10; Accelrys, Inc.: San Diego, CA.
(60) Rajapakse, C. S. K.; Martínez, A.; Naoulou, B.; Jarzecki, A. A.; Suarez, L.; Deregnaucourt, C.; Sinou, V.; Schrevel, J.; Musi, E.; Ambrosini, G.; Schwartz, G. K.; Sánchez-Delgado, R. A. Synthesis, characterization, and in vitro antimalarial and antitumor activity of new ruthenium(II) complexes of chloroquine. *Inorg. Chem.* **2009**, *48*, 1122−1131.
(61) Sharma, P.; Chhabra, S.; Rai, N.; Ghoshal, N. Exploration of rate-limiting conformational state for 5-[(7-chloro-4-quinolinyl)-amino]-3-[(alkylamino)methyl][1,1-biphenyl]-2-ols and *N*-oxides (tebuquine analogues) for antimalarial activity using molecular shape analysis and molecular field analysis studies. *J. Chem. Inf. Model.* **2007**, *47*, 1087−1096.
(62) Veber, D. F.; Johnson, S. E.; Cheng, Y.-H.; Smith, B. R.; Ward, K. W.; Kopple, K. D. Molecular properties that influence the oral bioavailability of drug candidates. *J. Med. Chem.* **2002**, *45*, 2615−2623.
(63) Mannhold, R. *Molecular Drug Properties: Measurement and Prediction*; Wiley-VCH: Chichester, U.K., 2007.
(64) Clark, D. E.; Grootenhuis, P. D. J. Predicting passive transport in silico—history, hype, hope. *Curr. Top. Med. Chem.* **2003**, *3*, 1193−1203.
(65) Kotecha, J.; Shah, S.; Rathod, I.; Subbaiah, G. Prediction of oral absorption in humans by experimental immobilized artificial membrane chromatography indices and physicochemical descriptors. *Int. J. Pharm.* **2008**, *360*, 96−106.
(66) Böcker, A.; Bonneau, P. R.; Hucke, O.; Jakalian, A.; Edwards, P. J. Development of specific "drug-like property" rules for carboxylate-containing oral drug candidates. *ChemMedChem* **2010**, *5*, 2102−2113.
(67) Glidewell, C.; Royles, B. J. L.; Smith, D. M. A simple high-yielding synthesis of ferrocene-1′-diylbis-(methyltrimethylammonium iodide). *J. Organomet. Chem.* **1997**, *527*, 259−261.
(68) Natarajan, J. K.; Alumasa, J. N.; Yearick, K.; Ekoue-Kovi, K. A.; Casabianca, L. B.; de Dios, A. C.; Wolf, C.; Roepe, P. D. 4-*N*-, 4-*S*-, and 4-*O*-Chloroquine analogues: influence of side chain length and quinolyl nitrogen pKa on activity vs chloroquine resistant malaria. *J. Med. Chem.* **2008**, *51*, 3466−3479.
(69) Trager, W.; Jensen, J. B. Human malaria parasite in continuous culture. *Science* **1976**, *193*, 673−675.
(70) Makler, M. T.; Ries, J.; Williams, J. A.; Bancroft, J. E.; Piper, R. C.; Gibbins, B. L.; Hinrichs, D. J. Parasite lactate dehydrogenase as an assay for *Plasmodium falciparum* drug sensitivity. *Am. J. Trop. Med. Hyg.* **1993**, *48*, 739−741.